EGF and bFGF pre-treatment enhances neural specification and the response to neuronal commitment of MIAMI cells.

Gaëtan Delcroix, K.-M. Curtis, Paul Schiller, Claudia Montero-Menei

EGF and bFGF pre-treatment enhances neural specification and the response to neuronal commitment of MIAMI cells

Gaëtan J-R DELCROIX[1,2#], Kevin CURTIS[3,4#], Paul C. SCHILLER[3,4,5], Claudia N. MONTERO-MENEI[1,2]

# authors contributed equally to this work

[1]Inserm, U646, Angers, F49100 France

[2]Univ Angers, UMR-S646, Angers, F49100 France

[3]GRECC, Veterans Affairs Medical Center and Geriatrics Institute and Departments of Biochemistry & Molecular Biology[4] and Medicine[5], University of Miami Miller School of Medicine, Florida, USA

Gaëtan J-R DELCROIX: delcroix.gaetan@gmail.com

Kevin CURTIS: kevinmcurtis@gmail.com

Paul C. SCHILLER: PSchille@med.miami.edu

Corresponding author: Claudia N. Montero-Menei

Inserm U646, 10 rue André Boquel, Angers, France

Phone : +33(0)2.41.73.58.94

Fax : +33(0)2.41.73.58.53

E-mail : claudia.montero-menei@univ-angers.fr

ABSTRACT

Aims. Multipotent mesenchymal stromal cells raise great interest for regenerative medicine studies. Some MSC subpopulations have the potential to undergo neural differentiation, including MIAMI (Marrow Isolated Adult Multilineage Inducible) cells, which differentiate into neuron-like cells in a multi-step neurotrophin 3-dependent manner. Epidermal and basic fibroblast growth factors are often used in neuronal differentiation protocols for MSCs, but with a limited understanding of their role. In this study, we thoroughly assessed for the first time the capacity of these factors to enhance the neuronal differentiation of MSCs. *Materials & Methods.* We have characterized MIAMI cell neuronal differentiation program in terms of stem cell molecule expression, cell cycle modifications, acquisition of a neuronal morphology and expression of neural and neuronal molecules in the absence and presence of an EGF-bFGF pre-treatment. *Results.* EGF-bFGF pre-treatment down-regulated the expression of stemness markers *Oct4A, Notch1* and *Hes5,* whereas neural/neuronal molecules *Nestin, Pax6, Ngn2* and the neurotrophin receptor tyrosine kinase 1 & 3 were up-regulated. During differentiation, a sustained Erk phosphorylation in response to NT3 was observed, cells began to exit from the cell cycle and exhibit increased neurite-like extensions. In addition, neuronal *β3-tubulin* and *Neurofilament* expression was increased, a slight preoligodendrocyte engagement was noted, and no default neurotransmitter phenotype was observed. Overall, mesodermal markers were unaffected or decreased, while neurogenic/adipogenic *PPARγ2* was increased. *Conclusion.* EGF and bFGF pre-treatment enhances neural specification and the response to neuronal commitment of MIAMI cells, further increasing their potential use in adult cell therapy of the nervous system.

Keywords: Mesenchymal stromal cell, epidermal growth factor, basic fibroblast growth factor, neuronal development, cell therapy

Abbreviation list: bFGF: basic fibroblast growth factor; BSA: bovine serum albumin; DMEM: Dulbecco's modified Eagle's medium-high glucose; DPBS: Dulbecco's phosphate buffered saline; EGF: epidermal growth factor; FBS: foetal bovine serum; HBSS: Hank's Buffered Salt Solution; ICF: immunocytofluorescence; ITS: insulin-transferrin-selenium; MIAMI: marrow isolated adult multilineage inducible; MSC: marrow stromal cell; NSC: neural stem cell; NT3: neurotrophin 3; Ntrk: neurotrophic tyrosine kinase receptor; RT-qPCR: real-time quantitative polymerase chain reaction; SD: standard deviation; SEM: scanning electron microscopy; WB: western blot.

INTRODUCTION

Stem cells hold a great promise in regenerative medicine due to their capacity to self-replicate and to produce various differentiated cell types. Nevertheless, the contribution of each stem cell type has to be clearly evaluated in the context of a specific pathology. Among the different sources of stem cells, adult multipotent mesenchymal stromal cells (MSCs) are interesting for cell therapy studies due to their large differentiation potential and their immunoregulatory properties [1-7]. Moreover, their easy isolation from bone marrow and their self-renewal capacity may allow autologous grafts to be performed. A number of studies have shown that subpopulations of MSCs differentiate into neuron-like cells *in vitro*, either by genetic manipulation, with the help of co-culture systems or by using different inducer molecules and growth factors [8-10]. In regard of the difficulties in obtaining neural stem cells (NSCs) from adults and the inherent ethical problems linked with their isolation from foetal tissue, the identification of alternate sources of neuron-like cells for cell therapy in the central nervous system is of great importance [1].

MSCs transplanted in adult rat brains may respond to microenvironmental cues and a fraction of them differentiate into neuron-like cells [11-13]. In addition, MSCs, that can migrate towards sources of lesions in the brain [13-17], may also provide a functional improvement in animal models, either directly or indirectly by their ability to produce various growth factors [15, 18-20]. Finally, their administration in the central nervous system is feasible and seems to be safe in human subjects [21]. For all of these reasons, use of MSCs may become a clinically viable technology for cell therapy of the central nervous system that is not hindered by ethical and tissue rejection-related concerns. However, further investigations are still required, particularly with human MSCs, to clearly evaluate their neuronal differentiation potential.

In the present study, we have used a homogenous subpopulation of developmentally immature human MSCs termed MIAMI (Marrow Isolated Adult Multilineage Inducible) cells. They are small cells with a reduced cytoplasm, that express markers typical of embryonic stem cells and are capable of

differentiating *in vitro* into cell lineages derived from all three germ layers, as previously described [22]. Moreover, MIAMI cells, which are isolated and expanded under niche-like conditions, including a low oxygen tension environment, express the major receptor for hepatocyte growth factor, c-met [22], as well as a number of chemokine and growth factor receptors, that may enhance their migratory potential leading to an improved regenerative potential [23]. We recently reported a 3-step neurotrophin 3 (NT3)-dependent differentiation of these cells using a protocol that aims to mimic the differentiation program of NSCs at the molecular level. At the end of this process, 50-60 % of MIAMI cells became immature neuron-like cells with a fraction showing ionic channel activity but no action potential [24]. For convenience purpose, in this study, this process will be termed "neuronal differentiation". Based on these results, it appears necessary to improve the neuronal differentiation potential of MIAMI cells, as well as to better understand their behavior and the molecular mechanisms that direct it, in order to optimize their future use in cell therapy studies.

Epidermal growth factor and basic fibroblast growth factor (EGF and bFGF) are powerful mitogens and cell fate drivers for NSCs and neural precursor cells present in the developing and adult central nervous system, as well as for ES cell-derived neural precursors [25-30]. Interestingly, these factors may also permit the long-term proliferation of human mesencephalic precursors expanded under hypoxia [31], while bFGF may contribute to maintain the neurogenic niche *in vivo* [32]. It has been shown that MSCs, including MIAMI cells, may already express certain neural-related genes [33, 34], and it was therefore assumed that an EGF-bFGF exposure may further improve their *in vitro* neuronal differentiation. In MSCs, the expression of Nestin, a marker expressed by NSCs [35], was up-regulated after EGF and bFGF exposure under adherent [36] or non-adherent conditions prior to *in vitro* neurogenesis [37-39]. Furthermore, recent studies described the differentiation of MSCs, after a first-step treatment with EGF-bFGF, into dopamine producing cells leading to a functional improvement in a rat model of Parkinson's disease [40, 41]. However, a precise characterization of the impact of an EGF-bFGF pre-treatment, prior to MSC neuronal differentiation, by comparing to non pre-treated cells

and extensively analyzing several neuronal molecules is still lacking [36-39, 42]. It is therefore important to thoroughly assess the benefits of using EGF-bFGF pre-treatment prior to the induction of MSCs toward a neuronal lineage.

In this study, we first sought to assess the potential benefits of an EGF-bFGF pre-treatment in terms of neuronal lineage specification of MIAMI cells to further improve their neuronal differentiation *in vitro*. In addition, the effects of the EGF-bFGF pre-treatment was characterized and compared on MIAMI cells harvested from vertebral bodies or from iliac crest of living donors. As NT3 is essential for MIAMI cells neuronal-like differentiation, we also studied the effect of EGF-bFGF on the response of MIAMI cells to NT3, by evaluating the expression of the NT3 receptors and Erk phosphorylation involved in this transduction pathway. Neuronal differentiation involves the reduction of cell proliferation leading to post-mitotic cells, a process accompanied with a loss of stem cell molecules together with the acquisition of a neuronal morphology and the expression of neural and neuronal molecules. Therefore, we further analyzed the behavior of MIAMI cells, with or w/o pre-treatment, along the differentiation protocol in terms of neuronal morphology, proliferation, apoptosis and molecular expression pattern.

MATERIALS AND METHODS

Bone marrow harvesting, selection & expansion of MIAMI cells. Whole bone marrow was obtained from vertebral bodies (T1–L5) of a 3 year old male cadaveric donor who died of fatal traumatic injury (MIAMI #519) [22] or from iliac crest of a 20 year old male living donor (Lonza Walkersville, Maryland; MIAMI #3515), following guidelines for informed consent set by the University of Miami School of Medicine Committee on the Use of Human Subjects in Research. As previously described [22], isolated whole bone marrow cells were plated at a constant density of 10^5 cells/cm^2 in DMEM-low glucose media, containing 5 % fetal bovine serum (FBS) (Hyclone, South Logan, Utah) and antibiotics (AB) (100 U/mL penicillin, 0.1 mg/mL streptomycin, 0.25 µg/mL amphotericin B) (Sigma, St Quentin Fallavier, France) on a fibronectin (Sigma) substrate. Whole bone marrow cells, containing adherent and non-adherent cells, were incubated at 37°C under hypoxic conditions (3 % O_2, 5 % CO_2 and 92 % N_2). Seven days later, half of the culture medium was replaced. Fourteen days after the initial plating, the non-adherent cells were removed. Pooled colonies of adherent cells were carefully rinsed and plated at low density for expansion (100 cells/cm) on 1.25 ng/cm fibronectin. Cells were expanded in DMEM-low glucose (Gibco, Cergy Pontoise, France), 3 % FBS and AB (40 mL/175 cm flask) under hypoxic conditions. Cells were fed every 2-3 days by changing half the medium and split every 5 days, keeping 1/4 of old medium. Presented results were obtained with vertebral bodies-isolated MIAMI cells, unless otherwise stated.

Neural stem cells. For use as positive controls, foetal neuroepithelial progenitor cells were kindly provided by Dr. Micheline McCarthy (Dept. of Neurology, Univ. of Miami, Miller School of Medicine) and cultured as previously described [24].

EGF-bFGF pre-treatment. A 10 day EGF & bFGF pre-treatment was performed using either a low dose (5 ng/mL) or a high dose (20-50 ng/mL) of both EGF and bFGF (R&D Systems Europe, Lille, France) supplemented with 5 µg/mL heparin (Sigma) and a lipid mixture (working concentration of 510 nM lipoic, 70 nM linolenic and 150 nM linoleic acid, all from Sigma). Unless otherwise stated,

presented results were mainly obtained with 20 ng/mL of EGF-bFGF. To investigate the NT3 response of pre-treated cells, we checked the neurotrophin receptor expression in response to 0, 50 and a higher dose (100 ng/mL) of EGF-bFGF. As we already observed an effect at the intermediary dose (50 ng/mL), we continued with this dose for the detection of Erk/pErk. Briefly, cells were treated with NT3 (30 ng/mL) for 5, 10 and 15 minutes following a serum deprivation phase of 24 hours prior processing for western blotting.

MIAMI cells neuronal-like differentiation. This 3-step differentiation process was described in greater detail elsewhere [24]. Non pre-treated or EGF-bFGF pre-treated MIAMI cells passages 5 to 9 were seeded at 3000–4000 cells/cm^2 on a 2 µg/cm fibronectin-coated surface in DMEM F12 (GIBCO) supplemented with 20 % FBS, 10 ng/mL bFGF (for the non pre-treated), antibiotics and cultured for 24 h (Neural specification, step 1). At the end of the neural specification treatment, cells were washed and neuronal commitment (step 2) was induced by exposing the cells to 30 ng/ml NT3 (R&D Systems) in the presence of 1 mM β-mercaptoethanol (Sigma), for 2 days. Neuronal differentiation (step 3) was induced by rinsing and then exposing the cells to 100 µM butylated hydroxyanisole, 25 mM KCl, 2 mM valproic acid, 4 µM forskolin, 1 µM hydrocortisone, 5 µM insulin, 5 mM Hepes, 10 µM rolipram (all from Sigma), 30 ng/mL NT3, 10 ng/mL NGF (R&D Systems), and 30 ng/mL BDNF (R&D Systems) for 3 days. Use of insulin-transferrin-selenium and lipid media supplement (ITS+3) (Sigma) was also tested during the differentiation protocol (working concentrations of 10 µg/ml insulin, 5.5 µg/ml apotransferrin, 5 ng/ml sodium selenite, 4.7 ng/ml linoleic acid, 4.7 ng/ml oleic acid and 0.5 µg/ml BSA). Neuronal differentiation was performed at ambient atmospheric oxygen (21 % pO_2).

Intracellular labeling & flow cytometry. MIAMI cells were washed with DMEM-low glucose and detached with 10 mL Versene (Lonza) for 20 min at 37°C. After pelleting, cells were washed with DPBS and fixation was performed in 0.25 % formaldehyde (Sigma) for 30-60 minutes at 4°C. After fixation, cells were pelleted, permeabilized with 0.5 % Tween 20 (Sigma) in DPBS for 15 min at 37°C and then rinsed with DPBS, 2 % FBS, 0.02 % azide, 0.2 % Tween 20. Incubation with mouse anti-

Nestin antibody (1:15, clone 3k1, #ab6320, Abcam, Paris, France) or IgG1k isotypic antibody (#557273, BD Biosciences, Le Pont De Claix, France) in DPBS, 2 % FBS, 0.02 % azide was made for 1 h at 4°C. After washing, FITC-conjugated anti-mouse antibody (1:50, #F0479, Dako, Trappes, France) was added for 30 min at 4°C. The cells were washed and finally fixed in DPBS, azide, 0.7 % formaldehyde. Fluorescence signals were acquired with a FACScalibur flow cytometer (BD Biosciences) and data analysed with the Cellquest software (BD Biosciences). The background level was estimated using the fluorescence signal of the isotypic control. Human NSCs were used as a positive control.

Primer design & validation. The following experimental details were performed following the guidelines of the SCCAN core facility ("Service Commun de Cytométrie et d'Analyse Nucléotidique", Angers, France). Human sequences were determined using Pubmed nucleotide search (www.ncbi.nlm.nih.gov) and Ensembl (www.ensembl.org) websites. The online freeware Primer3 (http://frodo.wi.mit.edu/cgi-bin/primer3/primer3_www.cgi) was used for primer modelling, clustalw (www.ebi.ac.uk) to align nucleotidic sequences and nucleotide blast (www.ncbi.nlm.nih.gov) to confirm the specificity of the defined primer sequences. When possible, pairs of primers were designed across intron-spanning regions to avoid genomic DNA contamination. Sense and antisense desalted primer pairs (Eurogentec, Angers, France or Origen, USA) were mixed in RNAse free water at a final concentration of 5 µM and validated using cDNA from expanding or differentiated MIAMI cells, expanding or differentiated foetal neuroepithelial cells and commercial qPCR Human Reference cDNA (Clontech, Takara bio, Saint-Germain-en-Laye, France). The melting peak of the amplicon had to be narrow and unique, and its size and specificity was confirmed by electrophoresis. Finally, a serial dilution of the PCR product was re-amplified to draw a linear curve Ct=f (Quantity). The efficiency of the primer was calculated from the slope of the linear curve: $E=[10^{(-1/slope)}-1]x100$. Only primer pairs with an efficiency greater than 80 % were validated for use (table 1).

RT-qPCR. During expansion and at the various steps of the differentiation protocol, MIAMI cells were detached using trypsin-EDTA (Sigma) and washed in DPBS. Following the manufacturer's guidelines, cells were lysed in a 1% β-mercaptoethanol containing buffer and RNA extracted following a treatment by DNAse to remove any traces of genomic DNA (Total RNA isolation Nucleospin® RNA II, Macherey Nagel, Hoerdt, France). First strand cDNA synthesis was performed with a Ready-To-Go You-Prime First-Strand Beads® kit in combination with random hexamers (Amersham Biosciences, Orsay, France) using 1 µg RNA according to the manufacturer's guidelines. Following first strand cDNA synthesis, cDNAs were purified (Qiaquick PCR purification kit, Qiagen, Courtaboeuf, France) and eluted in 50 µL RNAse free water (Gibco). Five microliters of cDNA (1:20) were mixed with iQ SYBR Green Supermix (Biorad) and primer mix (0.2 µM) in a final volume of 15 µL. Amplification was carried on a Chromo4 thermocycler (Biorad) with a first denaturation step at 95°C for 3 min and 40 cycles of 95°C for 10 s, 55°C for 15 s and 72°C for 15 s. After amplification, a melting curve of the products determined the specificity of the primers for the targeted genes. A mean cycle threshold value (Ct) was obtained from 2 measurements for each cDNA. Several housekeeping genes, Glyceraldehyde-3-phosphate dehydrogenase (Gapdh, NM_002046), Hypoxanthine phosphoribosyltransferase 1 (Hprt1, NM_000194), Beta actin (Actb, NM_001101), 30S ribosomal protein S18 (Rps18, NM_001093779) and Heat shock 90 kD protein 1 beta (Hspcb, NM_007355) were tested for normalization. The GeNorm™ freeware (www.primerdesign.co.uk/geNorm.asp) was used to determine that Gapdh, Hprt1 & Hspcb were the three most stable housekeeping genes. The relative transcript quantity (Q) was determined by the delta cT method $Q=E^{(\text{Ct min in all the samples tested-Ct of the sample})}$ where E is related to the primer efficiency (E=2 if the primer efficiency=100 %). Relative quantities (Q) were normalized using the multiple normalization method described in Vandesompele et al. [43]. Q normalized = Q/(geometric mean of the 3 most stable housekeeping genes Q). In the University of Miami's facilities, normalization was performed in a similar manner with two housekeeping genes, Eukaryotic translational elongation factor 1 alpha (Ef1a, NM_001402) and Ribosomal protein L13a (RpL13a,

NM_01242). On figures, results are expressed as a percentage of change in the expression of the mRNA relative to the expression in expanding MIAMI cells ± average deviation (% change mRNA X= $[(Q_x - Q_{\text{expanding MIAMI cells}})/Q_{\text{expanding MIAMI cells}}] \times 100$).

Western blotting. Cell protein extracts were separated into Triton X-100 soluble and insoluble lysates. Protease inhibitor cocktail (Sigma) was added to both lysis buffers directly prior to use. The cell pellet was resuspended in buffer A [500 mM Tris HCl pH 6.8, 50 mM EGTA, 1 M KCl, 10 % Triton X-100 (all from Sigma)], triturated, vortexed and centrifugated at 13000 g for 20 minutes to pellet the Triton X-100 insoluble pellet. Buffer A containing the supernatant Triton X-100 soluble fraction was stored at -80°C. The Triton X-100 insoluble pellet was washed twice with buffer B [500 mM TrisHCl pH6.8, 50 mM EGTA, 850 mM sucrose, 10 % Triton X-100 (all from Sigma)] then centrifugated at 13000 g for 20 minutes. Buffer B was aspirated from the Triton X-100 insoluble pellet and the pellet was reconstituted in Laemmli buffer [10 % SDS, 500 mM Tris HCl pH 6.8, 4 % glycerol, 1 % ß-ME, bromophenol blue (all from Sigma)], boiled for 5 minutes and stored at -80°C. The protein concentration of the Triton X-100 pellet was determined using the BCA protein assay (Pierce, Rockford, IL, USA). Primary antibodies included rabbit anti-Ntrk1 (1:2000, polyclonal, #sc-118, Santa Cruz Biotechnology, Santa Cruz, CA, USA), mouse anti-Ntrk3 (1:500, clone 75213, #MAB3731, R&D Systems), mouse anti-pErk p44/42 (1:2000, #9106S, Cell Signaling Technology, Danvers, MA, USA), mouse anti-Erk p44/42 (1:2000, #9107, Cell Signaling Technology), goat anti-pTau (Ser396) (1:500, polyclonal, #sc-12414, Santa Cruz Biotechnology) & mouse anti-Tau (1:500, monoclonal, #sc-32274, Santa Cruz Biotechnology). Secondary antibodies used were sheep anti-mouse IgG-horseradish peroxidase (HRP) (1:2000, GE Healthcare, USA), goat anti-rabbit IgG-HRP and bovine anti-goat IgG-HRP (1:1000, both from Santa Cruz Biotechnology) depending on the primary antibody. 50 µg protein extracts were electrophoresed on 6 % or 10 % gels and transferred onto Immobilon-P 0.2 µM membranes (Millipore). Membranes were blocked with 5 % BSA-DPBS for 1 hour then incubated with primary antibody in 5 % BSA-DPBS. Secondary antibodies were diluted in DPBS alone and incubated

on the membrane for 45 minutes. Membranes were developed with ECL Plus Western Blot Detection System (GE Healthcare) and an AFP Imaging Mini-Medical Services Auto developer. Image analysis was completed using ImageJ (http://rsbweb.nih.gov/ij/). Coomasie blue staining of the blot was used to control the total amount of proteins loaded.

Caspase 3 assay. MIAMI cells were plated in 1.9 cm fibronectin-coated wells and Caspase 3 activity was assessed following the Caspase 3 assay kit (Sigma) guidelines. Briefly, positive controls were induced by exposing the cells to Staurosporine (1 µg/mL, Sigma) for 4 hours at 37°C. After apoptotic induction of the positive controls, cell culture medium of every well was replaced by assay buffer and frozen at -80°C. After thawing, Caspase 3 substrate (Ac-DEVD-AMC) was added and the solutions transferred to black plates (Greiner bio-one, Courtaboeuf, France). Fluorescence was read in a kinetic mode for 1 hour at room temperature using a Fluoroskan Ascent FL microplate reader (Thermo Fisher scientific, Illkirch, France) with excitation/emission wavelengths of 355 nm-460 nm, respectively. Caspase 3 activity was read from a 7-amino-4-methylcoumarin standard curve. Caspase 3 specificity of the fluorescent signal was assessed with the Caspase 3 inhibitor (Ac-DEVD-CHO). Every condition was performed in triplicate.

Immunocytofluorescence (ICF). Uninduced and induced cells at the end of step 2 (neuronal commitment) and step 3 (neuronal differentiation) of neuronal induction were used for Nestin, β3-Tubulin and NFM ICF. After washing the slides 3 times with DPBS, cells were fixed with 4 % paraformaldehyde at 4°C for 15 min and then permeabilized with 0.2 % Triton X-100 (Sigma) for 5 min. Slides were blocked with DPBS, 10 % normal goat serum (Sigma), 4 % bovine serum albumin (BSA) (Sigma) at room temperature for 45 min. After washing, slides were incubated overnight at 4°C with anti-NFM (1:50, clone NN18, #N5264, Sigma), anti-β3-Tubulin (1:1000, clone SDL.3D10, #T8660, Sigma) or anti-nestin (1:200, clone 10C2, #MAB5326, Chemicon, St Quentin en Yvelines, France) antibodies in DPBS, 4 % BSA, 0.2 % Triton X-100. Isotypic controls were made with IgG1k (clone MOPC-31C, #557273, BD Biosciences) and IgG2bk (clone 27-35, #555740, BD Biosciences).

After rinsing, the cells were incubated with the secondary biotinylated anti-mouse antibody (1:200, Abcys) in DPBS, 4 % BSA, 0.2 % Triton X-100 for 1 hour. Finally, after rinsing again and following incubation with streptavidin-FITC (1:50, #F0422, Dako) in DPBS for 40 min, the slides were mounted (Dako) and observed with a fluorescence microscope (Axioscop, Carl Zeiss, Le Pecq, France), a CoolSnap ES camera (Photometrics, Tucson, Arizona) and Metavue software (Roper Scientific, Evry, France).

Scanning electron microscopy (SEM). Cells were cultivated on glass slides, fixed with 2 % glutaraldehyde (Sigma) and post-fixed with 2 % osmium tetroxide. Cells were then dehydrated with increasing concentrations of ethanol (Sigma) and transferred into acetone (Sigma) prior drying in a Bal-Tec CPD 030 critical point dryer (Bal-Tec, Liechtenstein). Samples were finally coated with carbon and examined with a Jeol 6301F scanning electron microscope (Jeol, Croissy sur Seine, France) at 11 kV for backscattered images.

Oil red staining. Oil red o (Sigma) solution (0.36 %) was made in 60 % isopropanol (Sigma) and agitated overnight before filtration. Medium was removed and cells fixed with 4 % paraformaldehyde during 30 to 40 min. Cells were washed with DPBS and water before staining with oil red solution for 50 min. Samples were finally washed with water and observed with a bright field microscope (Axiovert 40 CFL, Carl Zeiss).

Statistical analysis. Data are presented as the mean value of three independent experiments ± standard deviation (SD), unless otherwise stated. Significant differences between samples were determined using a Student's t-test modified for small samples with $t'_0=(m_1-m_2)/\sqrt{(s_1/n_1+s_2/n_2)}$. Differences were considered significant if $|t'_0| > t_{k':0.05}$, with k' being the closer integer of the calculated $k=(s_1/n_1+s_2/n_2)/[(1/(n_1-1)(s_1/n_1))+(1/(n_2-1)(s_2/n_2))]$. Kruskal-Wallis test was used for multiple comparisons. Threshold P-value was set to 0.05.

RESULTS

Direct effects of MIAMI cell exposure to EGF-bFGF. EGF and bFGF receptors, *EGFR* and *FGFR1* respectively, were highly expressed when assessed by RT-qPCR, suggesting that MIAMI cells may respond to the stimuli induced by these factors. In the following section, we first focus on the direct effects induced in MIAMI cells by an EGF-bFGF exposure.

Expression of stem and early neural-related genes after EGF-bFGF treatment. RT-qPCR demonstrated that expanding MIAMI cells expressed the stemness marker *Oct4A,* which was down-regulated after treatment with EGF-bFGF for 10 days (2.5 ± 0.5 fold decrease). MIAMI cells also expressed a panel of early neural-related genes, including *Nestin, Microtubule-associated protein 1b (MAP1b*), *Musashi homolog 1 (Msi1), Notch1, Hairy and enhancer of split 5 (HES5), Paired box 6 (Pax6) & Neurogenin 2 (Ngn2)*. The expression of *Nestin* was stimulated (2.9 ± 0.8 fold increase) by the EGF-bFGF treatment and this was confirmed by flow cytometry and ICF with 5 and 20 ng/mL EGF-bFGF (fig. 1 A, B), while a higher concentration (50 ng/mL) did not further increase *Nestin* expression. Moreover, Nestin was detected in almost all non-treated or treated cells, but its expression always remained lower than for NSCs used as a positive control (data not shown). *Pax6* increased after 20 ng/mL EGF-bFGF treatment (1.8 ± 0.1 fold increase), whereas the expression of *Notch1*, which plays a role in the control of NSC proliferation, slightly decreased (1.4 ± 0.1 fold decrease). Expression of *HES5* decreased and became almost undetectable while *Ngn2* increased (2.1 ± 0.1 fold), possibly as a consequence of *Notch1* down-regulation. Importantly, expression of stem and early neural-related genes was similar for iliac crest-derived MIAMI cells isolated from an older individual, with equivalent changes induced in response to EGF-bFGF exposure. All these results illustrate an EGF-bFGF induced specification of the MIAMI cells towards a neural phenotype, independently from their anatomical site of origin, *i.e.* vertebral bodies or iliac crest.

Effects of EGF-bFGF on the NT3 transduction pathway. Analysis of the NT3 receptor, neurotrophin tyrosine receptor kinase 3 (Ntrk3), revealed that both the full length isoform (gp145, FL-Ntrk3) and the

tyrosine kinase deficient isoform (gp100, Tkd-Ntrk3) of Ntrk3 were up-regulated along with Ntrk1, after EGF-bFGF treatment (fig. 2A). However, EGF-bFGF treatment did not further up-regulate Ntrk3 expression in iliac-crest isolated MIAMI cells, which express relatively higher basal levels of this receptor. In these cells, NT3 stimulation (30 ng/mL) induced Erk1/2 phosphorylation (p42/p44), which peaked after 5 min, decreased after 10 min and was not detectable after 15 min of stimulation. EGF-bFGF treatment resulted in a more sustained phosphorylation of pErk1/2 (p42 and p44: $p \leq 0.05$), still present at 10 min of NT3 stimulation compared to non-treated cells (fig. 2B, C). This result shows a differential response to NT3 stimulation after EGF-bFGF treatment, suggesting that the pre-treatment may permit the cells to better respond to NT3 during the neuronal differentiation.

Effects of EGF-bFGF pre-treatment during neuronal differentiation. To better understand the effects of the EGF-bFGF treatment, we describe in this second section its effects on the neuronal differentiation potential of MIAMI cells.

Decreased proliferation during neuronal differentiation. The antiproliferative gene *p21* was up-regulated during EGF-bFGF treatment (10.2 ± 0.7 fold increase) and Trypan blue counting suggested that cell doubling rate was reduced after exposure to EGF-bFGF. This reduced cell doubling rate was also observed during differentiation when cells were pre-treated with 5 ng/mL EGF-bFGF, while cell doubling was almost abolished with 20 ng/mL EGF-bFGF pre-treatement (fig. 3A). *Notch1* expression, which was already down-regulated after EGF-bFGF treatment, further decreased during neuronal differentiation, both for non pre-treated and EGF-bFGF pre-treated cells (fig. 3B). Moreover, expression of the cell cycle markers *p21* & *Cyclin D1* at the RNA level confirmed the decreased proliferation observed during differentiation after pre-treatment (fig. 3C, D). Indeed, *p21* was low in non pre-treated cells, it increased during differentiation in 5 ng/mL pre-treated cells and it was already elevated after 20 ng/mL pre-treatment, prior to the beginning of the differentiation. Conversely, *Cyclin D1* expression was high in non pre-treated cells and increased during differentiation. In 5 ng/mL EGF-

bFGF pre-treated cells, *Cyclin D1* decreased during differentiation whereas it was always low in cells pre-treated with a higher dose of EGF-bFGF. Importantly, dead cells were never detected during neuronal differentiation, with or w/o pre-treatment. To further confirm that there was no contribution from apoptosis to the reduced proliferation rate observed, a Caspase-3 apoptosis assay was performed. No Caspase-3 activity was detected, strongly suggesting that MIAMI cells, pre-treated or not with EGF-bFGF, did not undergo detectable apoptosis. In addition, it is interesting to note that at the end of differentiation, non pre-treated and EGF-bFGF pre-treated cells were sensitive to an apoptotic stress induced by 1 µg/mL staurosporine (fig. 4A). When exposed to staurosporine, the cells exhibited an increased Caspase 3 activity as well as a retracted morphology and nucleus fragmentation (fig. 4, B & C). However, under expansion conditions, both non pre-treated and pre-treated MIAMI cells seemed to be resistant to the proapoptotic inducer staurosporine as Caspase-3 activity was never detected (fig. 4A).

Homogeneous cell morphology and induced neurite extensions. Under low density expansion conditions, MIAMI cells are very small, slightly bipolar cells with a reduced cytoplasm compared to traditional MSCs. When treated with a combination of EGF-bFGF, MIAMI cells exhibited an even more homogeneous morphology with a refractile body, compared to non treated cells (fig. 5A, B). In addition, EGF-bFGF pre-treatment resulted in important morphological changes reminiscent of neurons at the end of the differentiation protocol (step 3). During the six days of neuronal differentiation, the small MIAMI cells gradually extended, thereby acquiring a neuron-like morphology with long neurite-like extensions (fig 5C, D). The total cell length could achieve more that 400 µm at the end of the differentiation when the EGF-bFGF pre-treatment was applied (table 2). EGF-bFGF pre-treated cells were also thinner than non pre-treated cells (fig. 5C, D & table 2) and numerous connexions could be observed by SEM at the end of differentiation (fig. 5E, F). Similar morphological changes were observed during neuronal differentiation when pre-treating iliac crest-isolated MIAMI cells with the EGF-bFGF pre-treatment.

Improved neuronal expression pattern during neuronal differentiation. Nestin expression was up-regulated during pre-treatment and its expression decreased during differentiation as observed by ICF at the end of step 3 and even more drastically after 12 days of step 3 (data not shown). The pattern of expression of the early neuronal marker *β3-Tubulin* followed the neuronal developmental program only if cells were pre-treated with EGF-bFGF. *β3-Tubulin* mRNA increased during neuronal differentiation before decreasing at the end of step 3 (fig. 6A). Moreover, its expression was already high after pre-treatment compared to non pre-treated cells. Using ICF, β3-Tubulin expression at the end of step 2 and 3 was always significantly higher for EGF-bFGF pre-treated cells compared to non pre-treated cells, both in terms of the percentage of β3-Tubulin expressing cells and marker intensity (fig. 6B, E). In addition, assessment of β3-Tubulin expression at the end of step 2 by ICF confirmed that removal of NT3 lowered the percentage of β3-Tubulin-positive cells at the end of step 2 (data not shown) as previously described [24], further supporting the role of NT3 on the neuronal differentiation of MIAMI cells.

The mRNA expression of the mature neuronal marker *Neurofilament medium* (*NFM)* underwent a strong decrease at the end of step 3 for non pre-treated cells. In contrast, expression of *NFM* increased throughout the differentiation protocol when the pre-treatment was used (fig. 6C). Similarly to β3-Tubulin, NFM protein expression was higher for pre-treated cells at the end of step 3 (fig. 6D, E). *Neurofilament light (NFL), NFM* and *Neurofilament heavy (NFH) mRNAs* were all up-regulated at the end of step 2 when iliac crest-isolated MIAMI cells were pre-treated with EGF-bFGF compared to non pre-treated cells (54.3 ± 9.3, 6.8 ± 0.2 & 2.0 ± 0.3 fold increase for *NFL, NFM* and *NFH*, respectively). Additionally, the unphosphorylated microtubule associated protein Tau, characteristic of immature neurons, was readily detectable throughout the neuronal differentiation procedure by Western blot analysis while we did not detect its phosphorylated form (data not shown). The major changes observed with and without EGF-bFGF pre-treatment before and during neuronal differentiation are summarized in table 3.

Neuronal neurotransmitter phenotypes during neuronal differentiation. Acetylcholinesterase (*AChE*), expressed by cholinergic and noradrenergic neurons, was detected at very low level by RT-qPCR during expansion and tended to increase during neuronal differentiation (10.4 ± 3.3 fold) when cells were pre-treated with EGF-bFGF. *Glutamate decarboxylase* (*GAD 25/67*), expressed by GABAergic neurons, *Choline acetyltransferase* (*ChAT*), another cholinergic phenotype enzyme and dopaminergic markers (*Tyrosine hydroxylase* (*TH*), *Dopamine transporter* (*DAT*) and *Nurr1)* were not detected or at very low levels.

Glial phenotypes during neuronal differentiation. Galactosylceramidase (*GalC*), characteristic of oligodendrocytes, was slightly expressed by MIAMI cells and further increased during neuronal differentiation for pre-treated cells, whereas its expression does not significantly vary in non pre-treated cells (fig. 7A). In opposition, *Oligodendrocyte lineage transcription factor 2 (Olig2),* another early marker of oligodendrocytes, was never detected in MIAMI cells. *Glial fibrillary acidic protein* (*GFAP*), specific of astrocytes, was not detected at the end of the differentiation. Previous results suggested that an insulin, transferin, selenium and lipids complement (ITS+3) improved cell morphology and membrane potential when used in step 3 (data not shown). However, when cultured in this lipid rich medium all along the differentiation protocol, numerous perinuclear lipid vesicles appeared at the end of step 2 and remained until the end of step 3, in a more significant manner for pre-treated cells, as observed with oil red staining (fig. 7C, D). The lipid nature of these vesicles was confirmed using back-scattered electron SEM imaging (fig. 7B), with visualization of osmium on double bonds-molecules rich sites.

Mesodermal phenotypes during neuronal differentiation. We analysed the expression of several genes related to mesodermal phenotypes, the major differentiation pathways of MSCs. *Sox9*, specific to chondrogenic progenitors, was slightly up-regulated during neuronal differentiation of non pre-treated cells (1.5 ± 0.1 fold increase); whereas it was down-regulated when cells were pre-treated with EGF-bFGF (2.5 ± 0.6 fold decrease), thereby underlining the importance of the pre-treatment for neuronal

differentiation purposes. The osteo-chondro marker *Runt-related transcription factor 2* (*Runx2*) was always detected at very low levels, while the osteogenic marker *Osterix* (*Sp7*) was never detected. *Peroxisome proliferator-activated receptor gamma* (*PPAR gamma)*, commonly related to the adipogenic/neurogenic lineage, was expressed by MIAMI cells. It was further up-regulated during differentiation, without significant changes with or w/o pre-treatment (11.4 ± 4.0 fold increase) whereas the solely adipogenic *Lipoprotein lipase (LpL)* was never detected. Noteworthy, exposure to ITS+3 during neuronal differentiation, described in the previous section, did not affect *PPAR gamma* expression and *LpL* remained undetected.

DISCUSSION

The differentiation of MSC subpopulations into neuron-like cells, a tightly controlled process involving a series of stimuli, has been recently reviewed [9]. In order to be able to use these cells for regenerative medicine studies in the brain, it is important to have a deeper understanding of the molecular events mediating this process. We have demonstrated that an EGF-bFGF treatment of human MIAMI cells, a subpopulation of MSCs, initiated their cell cycle exit and directed their gene expression pattern towards a neural/neuronal lineage. In addition, we reported in a previous study that NT3 was essential for the differentiation of MIAMI cells to cells with morphological, biochemical and electrophysiological characteristics of immature neurons [24]. In the present study, we observed that Ntrk1 and Ntrk3 receptors, both mediators of NT3 responses [44, 45], were up-regulated after EGF-bFGF treatment, a process accompanied with a more sustained phosphorylation of Erk in response to NT3. In this way, EGF-bFGF treatment enables the cells to better respond to the neuronal differentiation stimuli. We effectively observed that, during the induction protocol, EGF-bFGF pre-treated MIAMI-derived neuron-like cells stopped proliferating, presented longer neurite extensions and acquired an expression pattern more consistent with a neuronal differentiation program. These results shed light on the molecular events induced by an EGF-bFGF pre-treatment during the neuronal differentiation of MSC subpopulations. Thus, this pre-treatment may increase the benefit of using MSCs for regenerative medicine approaches of the nervous system.

MIAMI cells have a broad differentiation potential, express embryonic markers, including Rex1 and SSEA synthase [22, 24], as well as Oct4A, described as essential for the pluripotency and self-renewal properties of stem cells [46-48]. The latter was down-regulated over EGF-bFGF exposure, suggesting a certain commitment of the cells towards a differentiation program as previously suggested [37]. In this regard, a recent study demonstrates that Oct4 is required and sufficient to directly reprogram NSCs to pluripotency [49]. Nestin expression by pluripotent stem cells is considered to be a prerequisite for the commitment of the cells toward the neural lineage [50, 51] and this intermediate

filament protein is commonly used to identify NSCs and neural precursors [35], even if its expression may be found in other cell types. Using flow cytometry, all MIAMI cells were found to express Nestin, as reported in other studies although results vary depending on the detection method, cell species and expansion method used [24, 33, 36, 37, 51]. EGF-bFGF pre-treatment induced Nestin over-expression by MIAMI cells, as previously described for adherent or floating MSCs [37, 42, 50]; a mechanism that may be mediated through Erk pathway [52].

Notch1, which is involved in proliferation and maintenance of an undifferentiated state by NSCs [53], was down-regulated in response to EGF-bFGF treatment. Notch1 down-regulation could have led to the observed decreased expression of HES5 after EGF-bFGF pre-treatment [53]. Characteristic of decreased HES5 expression is the up-regulation of the early neuronal marker Ngn2 [53], which we also observed after EGF-bFGF treatment. Noteworthy, this response has previously been described in Nestin expressing cells after treatment with bFGF [54]. Pax6, known to promote neurogenesis in neural stem cells [55] was also up-regulated after pre-treatment. These results suggest a potential progression of MIAMI cells towards a neuronal phenotype.

Cell cycle gene analysis and cell counting confirmed the propensity of EGF-bFGF pre-treated cells to decrease their proliferation rate during neuronal differentiation. Indeed, non pre-treated cells exhibited a high level of Cyclin D1, the key cell-cycle regulatory protein governing progression from the G1 to S phase, and low level of the antiproliferative gene p21, a Cyclin-dependent kinase and Proliferating cell nuclear antigen (PCNA) inhibitor [56]. We can note that such a gene expression pattern is specific for integrin-mediated adhesion to fibronectin [57], the substrate used in this study. Conversely, p21 was up-regulated in pre-treated cells, and remained at high level during neuronal differentiation, while Cyclin D1 was down-regulated. These events, which take place during the exit from the cell cycle, have already been described in the context of terminal differentiation [58, 59]. In addition to its anti-proliferative role, p21 may rescue human MSCs from apoptosis induced by low density culture [60], with p21 loss increasing apoptosis [61]. In our study, we did not observe apoptotic

cells, neither in low density expansion nor in differentiation. However, differentiated MIAMI cells became sensitive to the pro-apoptotic molecule used as a positive control, confirming a previous report made with MSCs [62]. To explain this phenomenon, we may hypothesize that inhibition of Caspase 3, or of another related molecule, occurs in expansion and that this inhibition is abolished during differentiation. For example, the Heat shock protein Hsp20, highly expressed by MIAMI cells (data not shown), has recently been described to inhibit Caspase 3 via an interaction with the pro-apoptotic protein Bax [63, 64].

Altogether, these results demonstrate that EGF-bFGF treatment induces the specification of MIAMI cells toward the neural lineage. During neuronal differentiation, cells exhibited a strong propensity to exit from the cell cycle, which suggests that they are on their way to ultimately become post-mitotic. Moreover, the neuronal gene expression pattern closely mimicked the neuronal developmental program. *In vivo*, Nestin is down-regulated during the switch from neural precursors to differentiated post-mitotic neurons [35, 65], similarly to what we observed during differentiation of MIAMI cells by ICF. During the neuronal differentiation of pre-treated MIAMI cells, β3-Tubulin expression pattern was also similar to that of neuronal precursors, with a first increase followed by a terminal decrease at the end of the neuronal differentiation protocol [66]. NFL, NFM and NFH expression increased during neuronal differentiation, therefore following the expression pattern observed during normal brain development [67], whereas NFM decreased strongly at the end of step 3 for non pre-treated cells. In support of these results, we observed by ICF that EGF-bFGF pre-treatment resulted in a stronger expression of NFM and to a certain extent β3-Tubulin at the end of step 3. Pre-treated cells exhibited narrower and longer neurite-like extensions consistent with the filamentous protein expression. Therefore, EGF-bFGF pre-treatment enhanced the neuronal differentiation ability of MIAMI cells, although a fully mature phenotype was still not obtained as the neuronal marker Tau was not detected in its phosphorylated form. Without specific phenotype inducers, EGF-bFGF pre-treatment did not direct the neuronal differentiation toward a default neuronal pathway as mature

neurotransmitter markers were only slightly detected. However, we previously demonstrated that MIAMI cells were able to differentiate toward the dopaminergic phenotype in response to the correct instructive cues, *i.e.* sonic hedgehog, fibroblast growth factor 8 and retinoic acid [24].

For central nervous system cell therapy purposes, it is important to ascertain that MIAMI cells not only acquire a neuronal phenotype but also loose their mesodermal differentiation potential. In this study, differentiated MIAMI cells did not express osteogenic and adipogenic specific genes while the EGF-bFGF pre-treatment induced a decreased expression of Sox9, present in chondrogenic progenitors [68]. Only PPAR gamma was up-regulated during differentiation, a marker commonly related to the adipogenic but also neurogenic lineages [50, 69-71], thereby playing a role in proliferation and differentiation of NSCs [70, 71]. Moreover, lipid droplets were never observed inside the cells, unless if differentiated in a lipid rich medium supplemented with insulin, transferin and selenium, commonly used for neuronal differentiation purposes [36, 72-75]. PPAR gamma expression and the ability to uptake lipids are also observed in oligodendrocyte cell lines [76]. In this regard, the increased ability of differentiated EGF-bFGF pre-treated cells to produce lipid vesicles may be related to the observed up-regulation of the oligodendrocyte specific gene GalC even if Olig 2, mainly involved in the development of oligodendrocyte lineage [77], was never detected. In addition, Notch1 down-regulation renders possible the oligodendrocytic differentiation of NSCs [78], suggesting that MIAMI cells may commit toward a neuronal and preoligodendrocytic lineage after EGF-bFGF pre-treatment. In this respect, it has been proposed that some neurons and oligodendrocytes may share common progenitors during central nervous system development [79].

CONCLUSIONS

These results show that EGF-bFGF pre-treatment of MIAMI cells specified the cells toward the neural lineage and improved their neuronal differentiation program *in vitro*. In opposition to our method, others described culture of MSC spheroids in an EGF-bFGF containing medium prior to neuronal differentiation, but many of the cells died in the process of sphere formation [37]. Importantly, MIAMI cells isolated from the iliac crest of living donors exhibited similar responses to EGF-bFGF pre-treatment than MIAMI cells isolated from vertebral bodies, therefore allowing a simplified harvesting for autologous transplantation in clinical protocols. To our knowledge, this study is the first to precisely characterize the effects of an EGF-bFGF priming on human MSCs prior to neuronal differentiation. The results underline the advantages of pre-treating human MSCs with EGF-bFGF for neuronal differentiation purposes. In the future, EGF-bFGF pre-treatment may become an attractive, and easy to implement, method for enhancing the benefits of nervous system cell therapy based on the use of MSCs.

ACKNOWLEDGMENTS

We thank the SCIAM (Service Commun d'Imagerie et d'Analyse Microscopique) of Angers for SEM images. We would also like to thank Laurence Preisser (SCCAN, “Service Commun de Cytométrie et d'Analyse Nucléotidique”, Angers), Laurence Sindji, David Vazquez, and Nubia Rodriguez for their precious technical assistance, as well as Dr. Micheline McCarthy (Dept. Of Neurology, Univ. Of Miami) for supplying foetal neuroepithelial progenitor cells. This work was supported by the “Institut National de la Santé et de la Recherche Médicale”, the “Région Pays de la Loire” and by grants from the Department of Veterans Affairs, USA.

THERE IS NO DISCLOSURE OF INTEREST IN THIS PUBLICATION

REFERENCES

[1] G.J.R. Delcroix, P.C. Schiller, J.-P. Benoit, C.N. Montero-Menei, Adult cell therapy for brain neuronal damages and the role of tissue engineering, Biomaterials, 31 (2010) 2105-2120.

[2] K. Le Blanc, C. Tammik, K. Rosendahl, E. Zetterberg, O. Ringden, HLA expression and immunologic properties of differentiated and undifferentiated mesenchymal stem cells, Exp Hematol, 31 (2003) 890-896.

[3] K. Le Blanc, Immunomodulatory effects of fetal and adult mesenchymal stem cells, Cytotherapy, 5 (2003) 485-489.

[4] B. Maitra, E. Szekely, K. Gjini, M.J. Laughlin, J. Dennis, S.E. Haynesworth, O.N. Koc, Human mesenchymal stem cells support unrelated donor hematopoietic stem cells and suppress T-cell activation, Bone Marrow Transplant, 33 (2004) 597-604.

[5] A. Nasef, N. Mathieu, A. Chapel, J. Frick, S. Francois, C. Mazurier, A. Boutarfa, S. Bouchet, N.C. Gorin, D. Thierry, L. Fouillard, Immunosuppressive effects of mesenchymal stem cells: involvement of HLA-G, Transplantation, 84 (2007) 231-237.

[6] C. Gotherstrom, O. Ringden, C. Tammik, E. Zetterberg, M. Westgren, K. Le Blanc, Immunologic properties of human fetal mesenchymal stem cells, Am J Obstet Gynecol, 190 (2004) 239-245.

[7] E.M. Horwitz, K. Le Blanc, M. Dominici, I. Mueller, I. Slaper-Cortenbach, F.C. Marini, R.J. Deans, D.S. Krause, A. Keating, Clarification of the nomenclature for MSC: The International Society for Cellular Therapy position statement, Cytotherapy, 7 (2005) 393-395.

[8] A. Hermann, M. Maisel, A. Storch, Epigenetic conversion of human adult bone mesodermal stromal cells into neuroectodermal cell types for replacement therapy of neurodegenerative disorders, Expert Opin Biol Ther, 6 (2006) 653-670.

[9] J.J. Ross, C.M. Verfaillie, Evaluation of neural plasticity in adult stem cells, Philos Trans R Soc Lond B Biol Sci, 363 (2008) 199-205.

[10] S. Song, J. Sanchez-Ramos, Brain as the Sea of Marrow, Exp Neurol, 184 (2003) 54-60.

[11] G.C. Kopen, D.J. Prockop, D.G. Phinney, Marrow stromal cells migrate throughout forebrain and cerebellum, and they differentiate into astrocytes after injection into neonatal mouse brains, Proc Natl Acad Sci U S A, 96 (1999) 10711-10716.

[12] L.R. Zhao, W.M. Duan, M. Reyes, C.D. Keene, C.M. Verfaillie, W.C. Low, Human bone marrow stem cells exhibit neural phenotypes and ameliorate neurological deficits after grafting into the ischemic brain of rats, Exp Neurol, 174 (2002) 11-20.

[13] P. Jendelova, V. Herynek, L. Urdzikova, K. Glogarova, J. Kroupova, B. Andersson, V. Bryja, M. Burian, M. Hajek, E. Sykova, Magnetic resonance tracking of transplanted bone marrow and embryonic stem cells labeled by iron oxide nanoparticles in rat brain and spinal cord, J Neurosci Res, 76 (2004) 232-243.

[14] G.J. Delcroix, M. Jacquart, L. Lemaire, L. Sindji, F. Franconi, J.J. Le Jeune, C.N. Montero-Menei, Mesenchymal and neural stem cells labeled with HEDP-coated SPIO nanoparticles: in vitro characterization and migration potential in rat brain, Brain Res, 1255 (2009) 18-31.

[15] A. Mahmood, D. Lu, L. Wang, M. Chopp, Intracerebral transplantation of marrow stromal cells cultured with neurotrophic factors promotes functional recovery in adult rats subjected to traumatic brain injury, J Neurotrauma, 19 (2002) 1609-1617.

[16] E. Sykova, P. Jendelova, In vivo tracking of stem cells in brain and spinal cord injury, Prog Brain Res, 161 (2007) 367-383.

[17] M.A. Hellmann, H. Panet, Y. Barhum, E. Melamed, D. Offen, Increased survival and migration of engrafted mesenchymal bone marrow stem cells in 6-hydroxydopamine-lesioned rodents, Neurosci Lett, 395 (2006) 124-128.

[18] J. Zhang, Y. Li, J. Chen, Y. Cui, M. Lu, S.B. Elias, J.B. Mitchell, L. Hammill, P. Vanguri, M. Chopp, Human bone marrow stromal cell treatment improves neurological functional recovery in EAE mice, Exp Neurol, 195 (2005) 16-26.
[19] X. Chen, Y. Li, L. Wang, M. Katakowski, L. Zhang, J. Chen, Y. Xu, S.C. Gautam, M. Chopp, Ischemic rat brain extracts induce human marrow stromal cell growth factor production, Neuropathology, 22 (2002) 275-279.
[20] Y. Li, J. Chen, X.G. Chen, L. Wang, S.C. Gautam, Y.X. Xu, M. Katakowski, L.J. Zhang, M. Lu, N. Janakiraman, M. Chopp, Human marrow stromal cell therapy for stroke in rat: neurotrophins and functional recovery, Neurology, 59 (2002) 514-523.
[21] O.Y. Bang, J.S. Lee, P.H. Lee, G. Lee, Autologous mesenchymal stem cell transplantation in stroke patients, Ann Neurol, 57 (2005) 874-882.
[22] G. D'Ippolito, S. Diabira, G.A. Howard, P. Menei, B.A. Roos, P.C. Schiller, Marrow-isolated adult multilineage inducible (MIAMI) cells, a unique population of postnatal young and old human cells with extensive expansion and differentiation potential, J Cell Sci, 117 (2004) 2971-2981.
[23] I. Rosova, M. Dao, B. Capoccia, D. Link, J.A. Nolta, Hypoxic preconditioning results in increased motility and improved therapeutic potential of human mesenchymal stem cells, Stem Cells, 26 (2008) 2173-2182.
[24] V.M. Tatard, G. D'Ippolito, S. Diabira, A. Valeyev, J. Hackman, M. McCarthy, T. Bouckenooghe, P. Menei, C.N. Montero-Menei, P.C. Schiller, Neurotrophin-directed differentiation of human adult marrow stromal cells to dopaminergic-like neurons, Bone, 40 (2007) 360-373.
[25] A. Bithell, S.E. Finch, M.F. Hornby, B.P. Williams, Fibroblast growth factor 2 maintains the neurogenic capacity of embryonic neural progenitor cells in vitro but changes their neuronal subtype specification, Stem Cells, 26 (2008) 1565-1574.
[26] R.Y. Tsai, S. Kim, Fibroblast growth factor 2 negatively regulates the induction of neuronal progenitors from neural stem cells, J Neurosci Res, 82 (2005) 149-159.
[27] S. Temple, The development of neural stem cells, Nature, 414 (2001) 112-117.
[28] M.A. Caldwell, E. Garcion, M.G. terBorg, X. He, C.N. Svendsen, Heparin stabilizes FGF-2 and modulates striatal precursor cell behavior in response to EGF, Exp Neurol, 188 (2004) 408-420.
[29] K. Guan, H. Chang, A. Rolletschek, A.M. Wobus, Embryonic stem cell-derived neurogenesis. Retinoic acid induction and lineage selection of neuronal cells, Cell Tissue Res, 305 (2001) 171-176.
[30] B.A. Reynolds, W. Tetzlaff, S. Weiss, A multipotent EGF-responsive striatal embryonic progenitor cell produces neurons and astrocytes, J Neurosci, 12 (1992) 4565-4574.
[31] J. Schwarz, Developmental perspectives on human midbrain-derived neural stem cells, Parkinsonism Relat Disord, 13 Suppl 3 (2007) S466-468.
[32] G. Mudo, A. Bonomo, V. Di Liberto, M. Frinchi, K. Fuxe, N. Belluardo, The FGF-2/FGFRs neurotrophic system promotes neurogenesis in the adult brain, J Neural Transm, (2009).
[33] T. Tondreau, L. Lagneaux, M. Dejeneffe, M. Massy, C. Mortier, A. Delforge, D. Bron, Bone marrow-derived mesenchymal stem cells already express specific neural proteins before any differentiation, Differentiation, 72 (2004) 319-326.
[34] D. Woodbury, K. Reynolds, I.B. Black, Adult bone marrow stromal stem cells express germline, ectodermal, endodermal, and mesodermal genes prior to neurogenesis, J Neurosci Res, 69 (2002) 908-917.
[35] A.V. Gilyarov, Nestin in central nervous system cells, Neurosci Behav Physiol, 38 (2008) 165-169.
[36] S. Song, S. Song, H. Zhang, J. Cuevas, J. Sanchez-Ramos, Comparison of Neuron-Like Cells Derived from Bone Marrow Stem Cells to Those Differentiated from Adult Brain Neural Stem Cells, Stem Cells Dev, 16 (2007) 747-756.
[37] A. Hermann, R. Gastl, S. Liebau, M.O. Popa, J. Fiedler, B.O. Boehm, M. Maisel, H. Lerche, J. Schwarz, R. Brenner, A. Storch, Efficient generation of neural stem cell-like cells from adult human bone marrow stromal cells, J Cell Sci, 117 (2004) 4411-4422.

[38] S. Kim, O. Honmou, K. Kato, T. Nonaka, K. Houkin, H. Hamada, J.D. Kocsis, Neural differentiation potential of peripheral blood- and bone-marrow-derived precursor cells, Brain Res, 1123 (2006) 27-33.
[39] Q. Yang, J. Mu, Q. Li, A. Li, Z. Zeng, J. Yang, X. Zhang, J. Tang, P. Xie, A simple and efficient method for deriving neurospheres from bone marrow stromal cells, Biochem Biophys Res Commun, 372 (2008) 520-524.
[40] R. Barzilay, I. Kan, T. Ben-Zur, S. Bulvik, E. Melamed, D. Offen, Induction of human mesenchymal stem cells into dopamine-producing cells with different differentiation protocols, Stem Cells Dev, 17 (2008) 547-554.
[41] Y.S. Levy, M. Bahat-Stroomza, R. Barzilay, A. Burshtein, S. Bulvik, Y. Barhum, H. Panet, E. Melamed, D. Offen, Regenerative effect of neural-induced human mesenchymal stromal cells in rat models of Parkinson's disease, Cytotherapy, 10 (2008) 340-352.
[42] X. Long, M. Olszewski, W. Huang, M. Kletzel, Neural cell differentiation in vitro from adult human bone marrow mesenchymal stem cells, Stem Cells Dev, 14 (2005) 65-69.
[43] J. Vandesompele, K. De Preter, F. Pattyn, B. Poppe, N. Van Roy, A. De Paepe, F. Speleman, Accurate normalization of real-time quantitative RT-PCR data by geometric averaging of multiple internal control genes, Genome Biol, 3 (2002) RESEARCH0034.
[44] L.F. Reichardt, Neurotrophin-regulated signalling pathways, Philos Trans R Soc Lond B Biol Sci, 361 (2006) 1545-1564.
[45] L. Ivanisevic, W. Zheng, S.B. Woo, K.E. Neet, H.U. Saragovi, TrkA receptor "hot spots" for binding of NT-3 as a heterologous ligand, J Biol Chem, 282 (2007) 16754-16763.
[46] S. Masui, Y. Nakatake, Y. Toyooka, D. Shimosato, R. Yagi, K. Takahashi, H. Okochi, A. Okuda, R. Matoba, A.A. Sharov, M.S. Ko, H. Niwa, Pluripotency governed by Sox2 via regulation of Oct3/4 expression in mouse embryonic stem cells, Nat Cell Biol, 9 (2007) 625-635.
[47] L.A. Boyer, T.I. Lee, M.F. Cole, S.E. Johnstone, S.S. Levine, J.P. Zucker, M.G. Guenther, R.M. Kumar, H.L. Murray, R.G. Jenner, D.K. Gifford, D.A. Melton, R. Jaenisch, R.A. Young, Core transcriptional regulatory circuitry in human embryonic stem cells, Cell, 122 (2005) 947-956.
[48] S. Liedtke, M. Stephan, G. Kogler, Oct4 expression revisited: potential pitfalls for data misinterpretation in stem cell research, Biol Chem, 389 (2008) 845-850.
[49] J.B. Kim, V. Sebastiano, G. Wu, M.J. Arauzo-Bravo, P. Sasse, L. Gentile, K. Ko, D. Ruau, M. Ehrich, D. van den Boom, J. Meyer, K. Hubner, C. Bernemann, C. Ortmeier, M. Zenke, B.K. Fleischmann, H. Zaehres, H.R. Scholer, Oct4-induced pluripotency in adult neural stem cells, Cell, 136 (2009) 411-419.
[50] M. Shiota, T. Heike, M. Haruyama, S. Baba, A. Tsuchiya, H. Fujino, H. Kobayashi, T. Kato, K. Umeda, M. Yoshimoto, T. Nakahata, Isolation and characterization of bone marrow-derived mesenchymal progenitor cells with myogenic and neuronal properties, Exp Cell Res, 313 (2007) 1008-1023.
[51] S. Wislet-Gendebien, P. Leprince, G. Moonen, B. Rogister, Regulation of neural markers nestin and GFAP expression by cultivated bone marrow stromal cells, J Cell Sci, 116 (2003) 3295-3302.
[52] Y.L. Huang, G.Y. Shi, H. Lee, M.J. Jiang, B.M. Huang, H.L. Wu, H.Y. Yang, Thrombin induces nestin expression via the transactivation of EGFR signalings in rat vascular smooth muscle cells, Cell Signal, (2009).
[53] R. Kageyama, T. Ohtsuka, J. Hatakeyama, R. Ohsawa, Roles of bHLH genes in neural stem cell differentiation, Exp Cell Res, 306 (2005) 343-348.
[54] E. Vergano-Vera, H.R. Mendez-Gomez, A. Hurtado-Chong, J.C. Cigudosa, C. Vicario-Abejon, FGF-2 increases the expression of neurogenic genes and promotes the migration and differentiation of neurons derived from transplanted neural stem/progenitor cells, Neuroscience, (2009).
[55] T. Kallur, R. Gisler, O. Lindvall, Z. Kokaia, Pax6 promotes neurogenesis in human neural stem cells, Mol Cell Neurosci, 38 (2008) 616-628.

[56] Y. Luo, J. Hurwitz, J. Massague, Cell-cycle inhibition by independent CDK and PCNA binding domains in p21Cip1, Nature, 375 (1995) 159-161.
[57] E.H. Danen, K.M. Yamada, Fibronectin, integrins, and growth control, J Cell Physiol, 189 (2001) 1-13.
[58] E. Pacary, H. Legros, S. Valable, P. Duchatelle, M. Lecocq, E. Petit, O. Nicole, M. Bernaudin, Synergistic effects of CoCl(2) and ROCK inhibition on mesenchymal stem cell differentiation into neuron-like cells, J Cell Sci, 119 (2006) 2667-2678.
[59] S.V. Ekholm, S.I. Reed, Regulation of G(1) cyclin-dependent kinases in the mammalian cell cycle, Curr Opin Cell Biol, 12 (2000) 676-684.
[60] C. van den Bos, S. Silverstetter, M. Murphy, T. Connolly, p21(cip1) rescues human mesenchymal stem cells from apoptosis induced by low-density culture, Cell Tissue Res, 293 (1998) 463-470.
[61] J. Seoane, H.V. Le, J. Massague, Myc suppression of the p21(Cip1) Cdk inhibitor influences the outcome of the p53 response to DNA damage, Nature, 419 (2002) 729-734.
[62] M. Pelletier, L. Oliver, K. Meflah, F.M. Vallette, Caspase-3 can be pseudo-activated by a Ca2+-dependent proteolysis at a non-canonical site, FEBS Lett, 579 (2005) 2364-2368.
[63] G.C. Fan, G. Chu, E.G. Kranias, Hsp20 and its cardioprotection, Trends Cardiovasc Med, 15 (2005) 138-141.
[64] G.C. Fan, X. Ren, J. Qian, Q. Yuan, P. Nicolaou, Y. Wang, W.K. Jones, G. Chu, E.G. Kranias, Novel cardioprotective role of a small heat-shock protein, Hsp20, against ischemia/reperfusion injury, Circulation, 111 (2005) 1792-1799.
[65] L. Zimmerman, B. Parr, U. Lendahl, M. Cunningham, R. McKay, B. Gavin, J. Mann, G. Vassileva, A. McMahon, Independent regulatory elements in the nestin gene direct transgene expression to neural stem cells or muscle precursors, Neuron, 12 (1994) 11-24.
[66] I. Ginzburg, A. Teichman, H.J. Dodemont, L. Behar, U.Z. Littauer, Regulation of three beta-tubulin mRNAs during rat brain development, Embo J, 4 (1985) 3667-3673.
[67] P.F. Moskowitz, M.M. Oblinger, Transcriptional and post-transcriptional mechanisms regulating neurofilament and tubulin gene expression during normal development of the rat brain, Brain Res Mol Brain Res, 30 (1995) 211-222.
[68] O.J. Marshall, V.R. Harley, Molecular mechanisms of SOX9 action, Mol Genet Metab, 71 (2000) 455-462.
[69] L. Casteilla, B. Cousin, M. Carmona, PPARs and Adipose Cell Plasticity, PPAR Res, 2007 (2007) 68202.
[70] A. Cimini, M.P. Ceru, Emerging roles of peroxisome proliferator-activated receptors (PPARs) in the regulation of neural stem cells proliferation and differentiation, Stem Cell Rev, 4 (2008) 293-303.
[71] K. Wada, A. Nakajima, K. Katayama, C. Kudo, A. Shibuya, N. Kubota, Y. Terauchi, M. Tachibana, H. Miyoshi, Y. Kamisaki, T. Mayumi, T. Kadowaki, R.S. Blumberg, Peroxisome proliferator-activated receptor gamma-mediated regulation of neural stem cell proliferation and differentiation, J Biol Chem, 281 (2006) 12673-12681.
[72] S. Okabe, K. Forsberg-Nilsson, A.C. Spiro, M. Segal, R.D. McKay, Development of neuronal precursor cells and functional postmitotic neurons from embryonic stem cells in vitro, Mech Dev, 59 (1996) 89-102.
[73] J. Sanchez-Ramos, S. Song, F. Cardozo-Pelaez, C. Hazzi, T. Stedeford, A. Willing, T.B. Freeman, S. Saporta, W. Janssen, N. Patel, D.R. Cooper, P.R. Sanberg, Adult bone marrow stromal cells differentiate into neural cells in vitro, Exp Neurol, 164 (2000) 247-256.
[74] H. Tao, R. Rao, D.D. Ma, Cytokine-induced stable neuronal differentiation of human bone marrow mesenchymal stem cells in a serum/feeder cell-free condition, Dev Growth Differ, 47 (2005) 423-433.
[75] Y.S. Levy, D. Merims, H. Panet, Y. Barhum, E. Melamed, D. Offen, Induction of neuron-specific enolase promoter and neuronal markers in differentiated mouse bone marrow stromal cells, J Mol Neurosci, 21 (2003) 121-132.

[76] A.D. Roth, A.V. Leisewitz, J.E. Jung, P. Cassina, L. Barbeito, N.C. Inestrosa, M. Bronfman, PPAR gamma activators induce growth arrest and process extension in B12 oligodendrocyte-like cells and terminal differentiation of cultured oligodendrocytes, J Neurosci Res, 72 (2003) 425-435.
[77] I. Jakovcevski, N. Zecevic, Olig transcription factors are expressed in oligodendrocyte and neuronal cells in human fetal CNS, J Neurosci, 25 (2005) 10064-10073.
[78] S. Wang, A.D. Sdrulla, G. diSibio, G. Bush, D. Nofziger, C. Hicks, G. Weinmaster, B.A. Barres, Notch receptor activation inhibits oligodendrocyte differentiation, Neuron, 21 (1998) 63-75.
[79] D.H. Rowitch, Q.R. Lu, N. Kessaris, W.D. Richardson, An 'oligarchy' rules neural development, Trends Neurosci, 25 (2002) 417-422.

TABLES

Table 1. Human specific primer sequences

Gene	Full name	NM accession number	Sequences	Amplicon
AChE	*Acetylcholinesterase*	015831-00665	F=5'-CCCTCTCGAAACTACACG-3' R=5'-GGTCCAGACTAACGTACTGC-3'	163
β3-Tubulin	*Homo sapiens tubulin, beta 3*	006086	F=5'-CCAGTATGAGGGAGATCG-3' R=5'-CACGTACTTGTGAGAAGAGG-3'	185
CCND1	*Cyclin D1*	053056	F=5'-CTCTCCAAAATGCCAGAG-3' R=5'-GATGGACAGGAAGTTGTTGG-3'	186
ChAT	*Choline acetyltransferase*	020549-020984-020985-020986	HS_CHAT_1_SG QUANTITECT PRIMER ASSAY, REF QT00029624, QIAGEN	Unknown
DAT	*Dopamine transporter*	001044	F=5'-GAAGGTGGTATGGATCACAG-3' R=5'-GTAGAAGTCAACGCTCAGGT-3'	121
EGFR	*EGF receptor*	005228	F=5'-CAGCCACCCATATGTACC-3' R=5'-TGGAGTCTGTAGGACTTGG-3'	184
FGFR1	*FGF receptor 1*	015850-023105-023106-023110-023111	F=5'-GGTAACTCTATCGGACTCTCC-3' R=5'-GTGGAAGTCACTCTTCTTGG-3'	198
GAD 25/67	*Glutamate decarboxylase*	000817-013445	F=5'-CCTGGAAGAGAAGAGTCG-3' R=5'-CTCCTCACCGTTCTTAGC-3'	166
GalC	*Galactosylceramidase*	000153-001037525	F=5'-GTTGCCTTATGGGAGATG-3' R=5'-AAGCCATCAGTCAGAGGCTAC-3'	183
GFAP	*Glial fibrillary acidic protein*	002055	F=5'-TTGAGAGGGACAATCTGG-3' R=5'-CGACTCAATCTTCCTCTCC-3'	161
*HES5**	*Hairy and enhancer of split 5*	001010926	F=5'-AGCCCCAAAGAGAAAAACCGA-3' R=5'-GCTGTGCTTCAGGTAGCTGAC-3'	183
*LpL**	*Lipoprotein lipase*	000237	F=5'-ACAAGAGAGAACCAGACTCCAA-3' R=5'-AGGGTAGTTAAACTCCTCCTCC-3'	149
MAP1b	*Microtubule-associated protein 1b*	005909	F=5'-CCTCGAGACGTGATGAGTGA-3' R=5'-TTGGGCGTCAGAGAGAAGTT-3'	437
Msi1	*Homo sapiens musashi homolog 1*	002442	F=5'-AGGTGAAGGAGTGTCTGG-3' R=5'-TTCTTCGTTCGAGTCACC-3'	196
Nes	*Nestin*	006617	F=5'-AGAAACAGGGCCTACAGAG-3' R=5'-AAAGCTGAGGGAAGTCTTG-3'	170
*NFL**	*Neurofilament, light polypeptide*	006158	F=5'-ATGAGTTCCTTCAGCTACGAGC-3' R=5'-GGGCATCAACGATCCAGAGC-3'	198
NFM	*Neurofilament, medium polypeptide*	005382	F=5'-GACCTCAGCAGCTACCAG-3' R=5'-CTAGTCTCTTCACCCTCCAG-3'	170
*NFH**	*Neurofilament, heavy polypeptide*	021076	F=5'-GCAGTCCGAGGAGTGGTTC-3' R=5'-TAGCGTCTGTGTTCACCTTGG-3'	71
*Ngn2**	*Neurogenin 2*	024019	F=5'-CGCATCAAGAAGACCCGTAG-3' R=5'-GTGAGTGCCCAGATGTAGTTGTG-3'	173
Notch1	*Notch homolog 1, translocation-associated*	017617	F=5'-GACCTCATCAACTCACACG-3' R=5'-AGAAACAGGGGTGTCTCC-3'	198
*Nurr1 (NR4A2)**	*nuclear receptor subfamily 4, group A, member 2*	006186	F=5'-TTGCCAGATGCGCTTCGACG-3' R=5'-CCAACAGCCAGGCACTTCTG-3'	414
Oct4A	*Pou class 5 homeobox 1*	002701	F=5'-TGGAGAAGGAGAAGCTGGAGCAAAA-3' R=5'-GGCAGATGGTCGTTTGGCTGAATA-3'	186
*Olig2**	*Oligodendrocyte lineage transcription factor 2*	005806	F=5'-GCTGCGACGACTATCTTCCC-3' R=5'-GCCTCCTAGCTTGTCCCCA-3'	244
*Pax6**	*Paired box 6*	000280-001604-001127612	F=5'-AGGTATTACGAGACTGGCTCC-3' R=5'-TCCCGCTTATACTGGGCTATTT-3'	104
p21	*Cyclin-dependent kinase inhibitor 1A*	000389-078467	F=5'-GCAGAGGAAGACCATGTG-3' R=5'-CCTCTTGGAGAAGATCAGC-3'	171
PPAR gamma	*Peroxisome proliferator-activated receptor gamma*	138712-015869-138711-005037	F=5'-AACAGATCCAGTGGTTGC-3' R=5'-CTCCACAGACACGACATTC-3'	176
*Runx2**	*Runt-related transcription factor 2*	001024630-004348	F=5'-TCCTATGACCAGTCTTACCCCT-3' R=5'-GGCTCTTCTTACTGAGAGTGGAA-3'	190
*Sox9**	*Sex determining region Y-box 9*	000346	F=5'-GCCAGGTGCTCAAAGGCTA-3' R=5'-TCTCGTTCAGAAGTCTCCAGAG-3'	213
Sp7 (Osterix)*	*Sp7 transcription factor*	152860	F=5'-CCCAGGCAACACTCCTACTC-3' R=5'-GGCTGGATTAAGGGGAGCAAA-3'	175
*TH**	*Tyrosine hydroxylase*	199292-000360-199293	F=5'-CACCATCTAGAGACCCGGCC-3' R=5'-GCAATCAGCTTCCTGCGCTG-3'	290

Primers with an "*" were obtained from Origen, USA and experiments with these primers performed in Miami's facilities.

Table 2. Cell area and length at the end of differentiation

	Non pre-treated cells	EGF-bFGF pre-treated cells
Cell area (µm²)	4378 ± 665	2893 ± 499*
Cell length (µm ± SD)	289 ± 43	421 ± 50*

EGF-bFGF pre-treated cells exhibited a decreased cell area (*i.e.* a narrower cell body) and an increased cell length, due to the presence of long neurite-like extensions at the end of step 3. Data represent the average length of the 3 longer cells of 5 different images in a representative experiment. * Significantly different means at P=0.05.

Table 3. Major effects of MIAMI cells exposure to EGF-bFGF

		Markers	Down/up-regulation	Fold change (RT-qPCR)
EGF-bFGF treatment	**Trancription factors**	*Oct4a*	↓	2.5 ± 0.5
		Notch1	↓	1.4 ± 0.1
		Ngn2	↑	2.1 ± 0.1
		HES5	↓	Undetectable
		Pax6	↑	1.8 ± 0.1
	Filaments	*Nes*	↑	2.9 ± 0.8
	Cell cycle	*P21*	↑	10.2 ± 0.7
		CyclinD1	<>	NA
	Receptors	*Ntrk1*	↑	NA
		Ntrk3	↑	NA
		Tkd-Ntrk3	↑	NA
	Proliferation rate		↓	NA
Effects of EGF-bFGF pre-treatment during neuronal differentiation	**Filaments**	*β3-Tubulin*	↑	1.4 ± 0.3
		NFL	↑	54.3 ± 9.3
		NFM	↑	6.8 ± 0.2
		NFH	↑	2.0 ± 0.3
	Cell cycle	*P21*	<>	NA
		Cyclin D1	↓	6.7 ± 2.6
	Oligodendrocyte	*GalC*	↑	7.5 ± 4.6
	Proliferation rate		↓	NA

Exposure of MIAMI cells to EGF-bFGF resulted in the differential expression of a large panel of markers, as observed using RT-qPCR, western blot, flow cytometry and immunocytofluorescence, thereby suggesting a neural specification of the cells. When applicable, fold change calculated by RT-qPCR are mentioned. After EGF-bFGF pre-treatment and further exposure to the 3 steps neuronal induction media, an increased expression of various neuronal filamentous proteins was observed, compared to non pre-treated MIAMI cells. In addition, a reduced proliferation rate during neuronal differentiation was observed only with EGF-bFGF pre-treated MIAMI cells, in accordance with a high expression of *P21* and a down-regulation of *Cyclin D1*. Thus, these results show that EGF and bFGF pre-treatment enhance the response of MIAMI cells to neuronal commitment. Abbreviations: NA: not applicable.

FIGURE LEGENDS

Fig. 1. Nestin up-regulation during EGF-bFGF treatment. Nestin expression by MIAMI cells increased after exposure to EGF-bFGF. After treatment, expression by flow cytometry increased (A) and was confirmed by ICF (B). Depicted results were obtained from a representative experiment and differences were considered significant at P=0.05*.

Fig. 2. Representative Ntrk up-regulation and Erk sustained phosphorylation. During EGF-bFGF pre-treatment, expression by MIAMI cells of Ntrk1, Ntrk3 and Tkd-Ntrk3 receptors were strongly up-regulated (A). Total proteins were detected by Coomasie blue staining. In response to NT3 stimulation, Erk phosphorylation peaked after 5 minutes and decreased at 10 min for non pre-treated cells. After 50 ng/mL EGF-bFGF pre-treatment, pErk peaked at 5 minutes and remained at a high level at 10 minutes of NT3 stimulation, compared to non pre-treated cells. This sustained phosphorylation was similar for p42 and p44 (B, C). *Differences were considered significant at P=0.05. Abbreviations: Ntrk: neurotrophic tyrosine kinase receptor.

Fig. 3. Reduced cell proliferation and cell cycle exit during neuronal differentiation. Trypan blue exclusion (A) demonstrated that the number of cells increased during differentiation while almost no increase was detected with 20 ng/mL EGF-bFGF pre-treated MIAMI cells. Analysis of *Notch1* (B) and cell cycle genes (*p21* & *Cyclin D1*, C & D respectively) expressions tended to confirm the reduced cell proliferation and cell cycle exit observed during differentiation after pre-treatment. *Differences were considered significant at P=0.05.

Fig. 4. Caspase 3 activity. MIAMI cells lack significant Caspase 3 activity (A), unless if treated with 1 µg/mL staurosporine (an apoptosis inducer). This significant increase was detected only in differentiated cells whereas proliferative cells were resistant to staurosporine treatment. The top right bar of the histogram was obtained with a caspase 3 solution as a positive control. Picture B depicts morphology of pre-treated MIAMI cells after differentiation compared to the same cells after staurosporine exposure (C). Abbreviations: Ssp: staurosporine. *Significantly different medians at P=0.05. Scale bars: 100 µm.

Fig. 5. Induced neural/neuronal morphology after EGF-bFGF pre-treatment. Expanding MIAMI cells (A) were larger than EGF-bFGF treated cells, which were narrower and more refractile (B). At the end of neuronal differentiation, EGF-bFGF pre-treated cells exhibited longer neurites as observed after NFM ICF (D) compared to non pre-treated cells (C). Neurite-like extensions and inter-connexions of EGF-bFGF pre-treated cells are depicted on SEM images at the end of differentiation (E, F, respectively). Scale bars A-E: 100 µm; F: 5 µm.

Fig. 6. Improved β3-Tubulin and NFM expression pattern during neuronal differentiation. EGF-bFGF pre-treated cells exhibited an increase and a final decrease *of β3-Tubulin* mRNA expression during differentiation (A), as well as a constant increase in *NFM* mRNA (C), similarly to what is observed during neuronal development *in vivo*. At the protein level, β3-Tubulin and NFM expression were higher for pre-treated cells as observed by ICF in terms of marker intensity (B, D respectively). EGF-bFGF pre-treatment also resulted in an increased number of for B3-Tubulin and NFM-positive cells with a neuronal morphology (E). Presented ICF data were obtained from a representative experiment and differences were considered significant at P=0.05*.

Fig. 7. EGF-bFGF may prime MIAMI cells toward a pre-oligodendrocyte lineage. GalC expression by MIAMI cells slightly increased during differentiation after EGF-bFGF pre-treatment (A). Use of ITS+3 during the neuronal differentiation protocol led to the formation of lipid vesicles (B, D, white arrowheads), especially in EGF-bFGF pre-treated cells. In presence of ITS+3, MIAMI cells exhibited red vesicles (D) at the end of differentiation compared to control cells (C) as observed with oil red staining. The lipid nature of the vesicles observed in EGF-bFGF pre-treated cells was confirmed by SEM. Osmium specifically links to double bounds-molecules such as lipids and back-scattering imaging reveals the localization of the osmium inside the cells (B). Scale bars B: 20 µm ; C, D: 100 µm.

Figure 1
Click here to download high resolution image

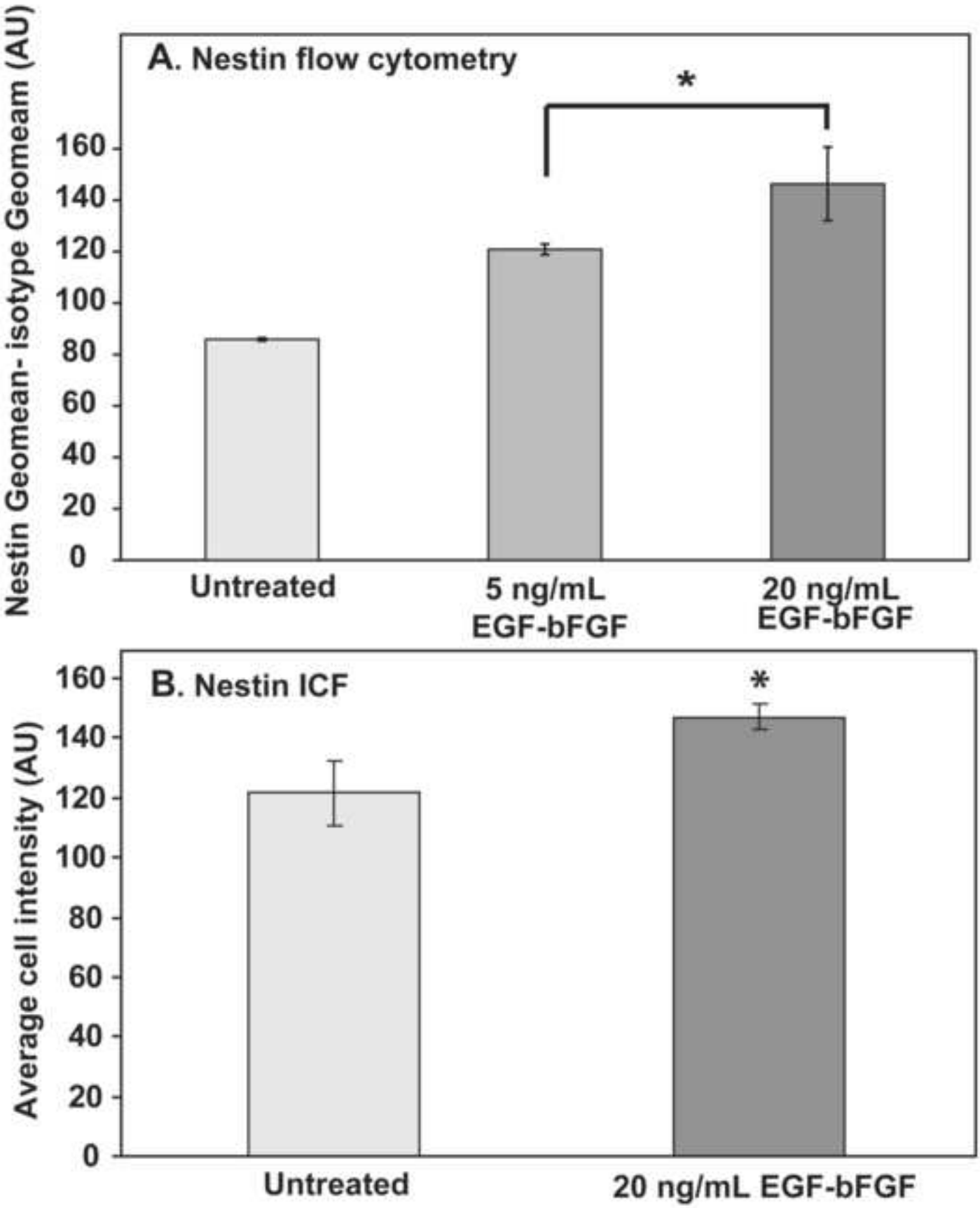

Figure 2

Click here to download high resolution image

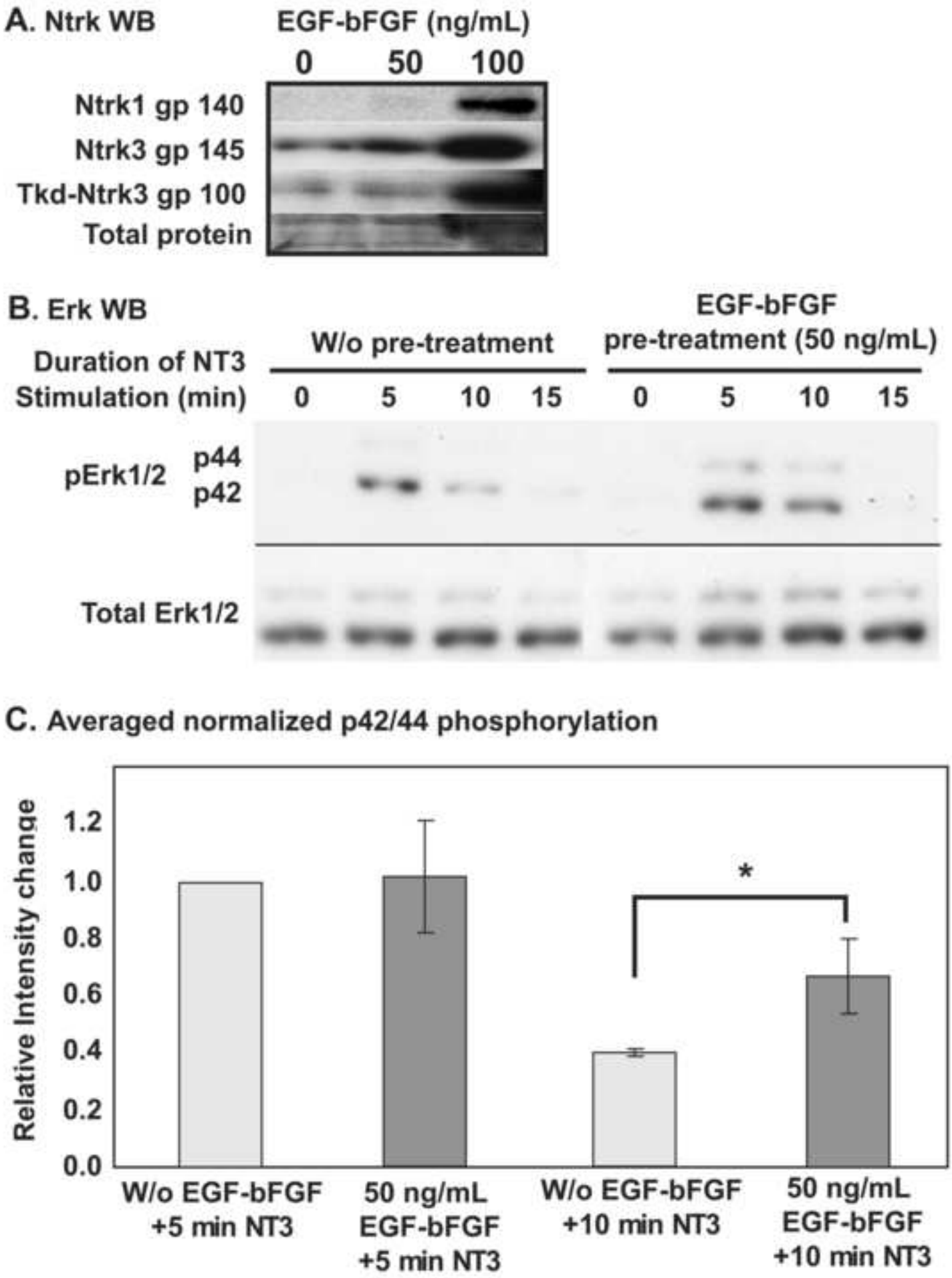

Figure 3

Click here to download high resolution image

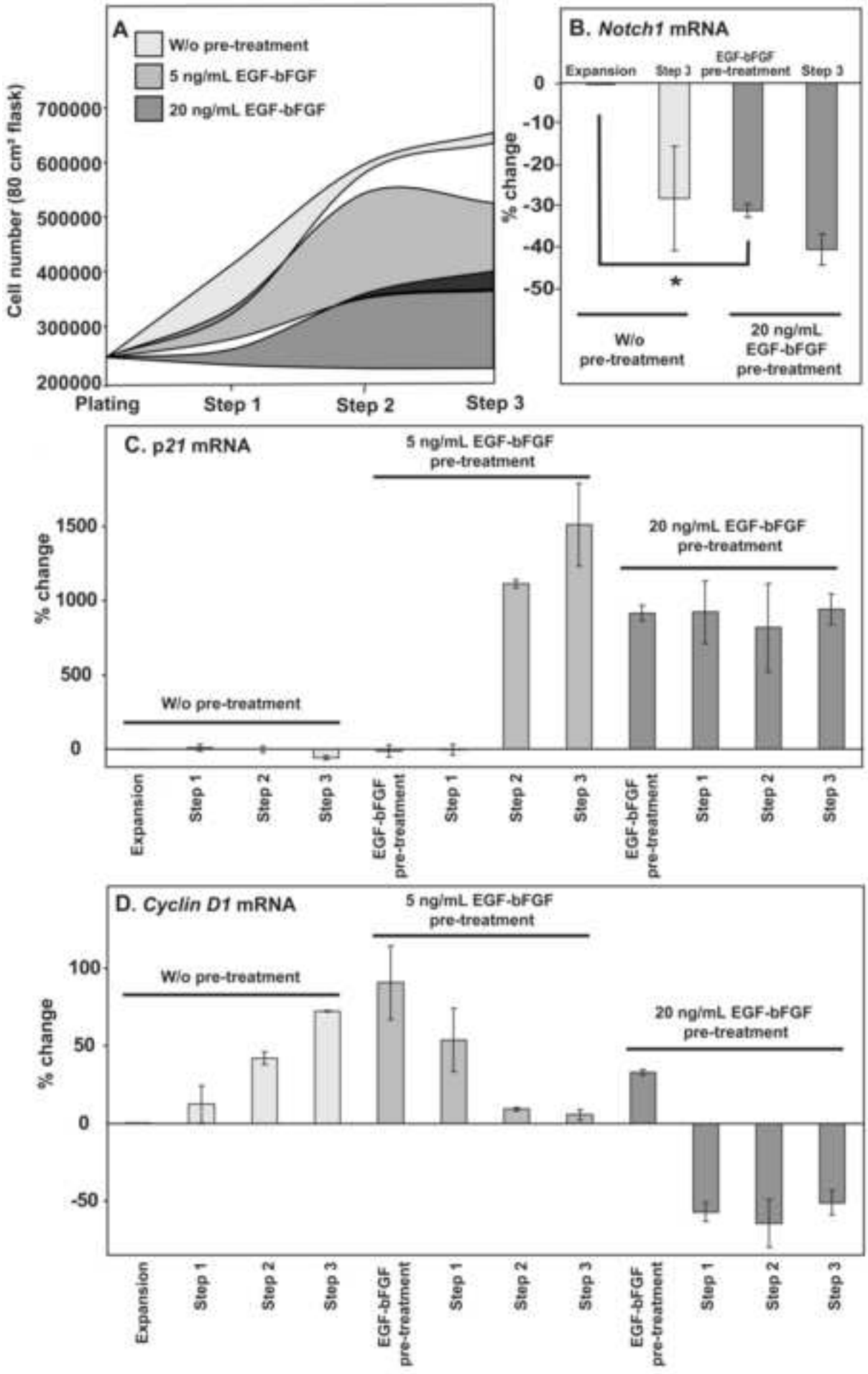

Figure 4

Click here to download high resolution image

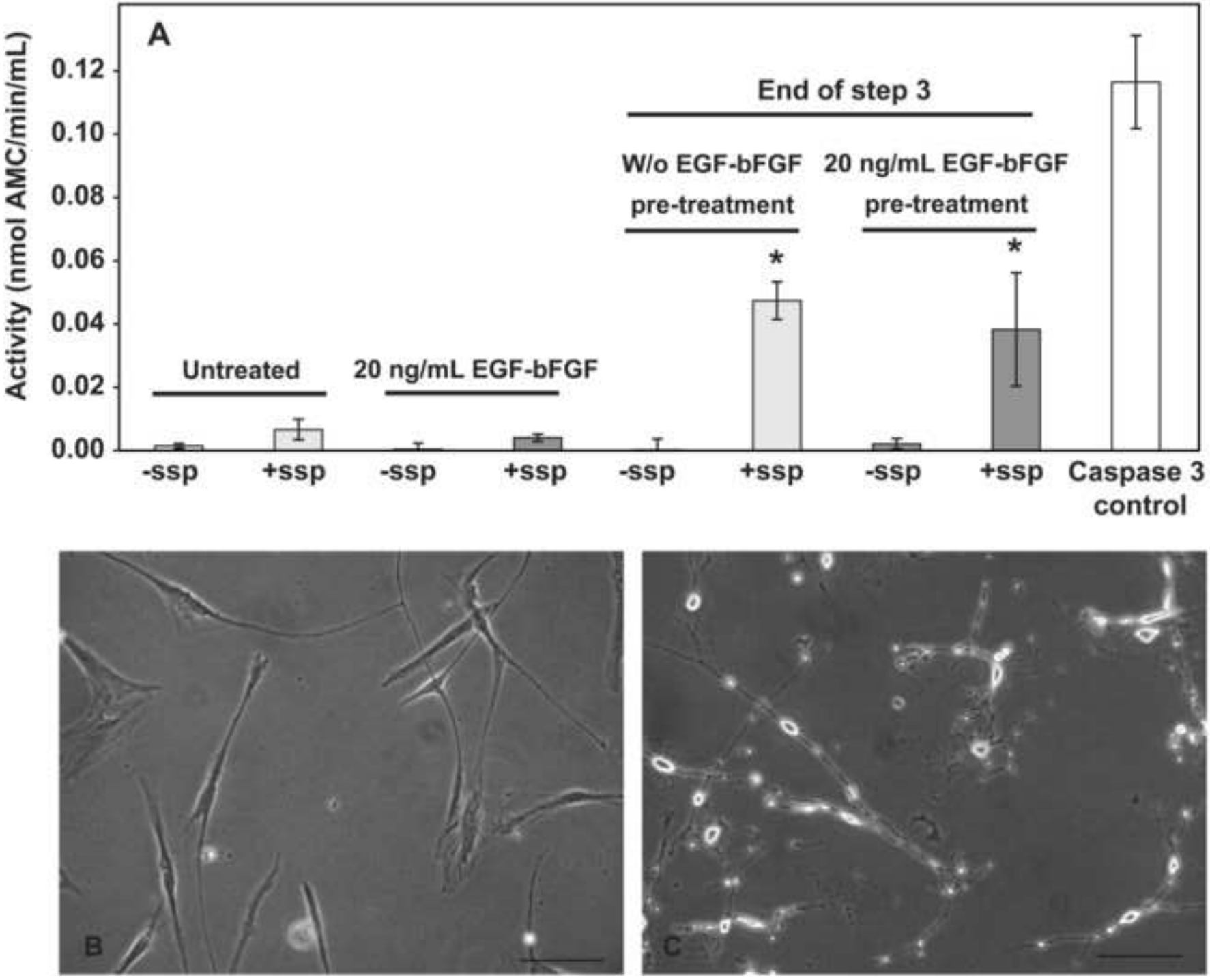

Figure 5

Click here to download high resolution image

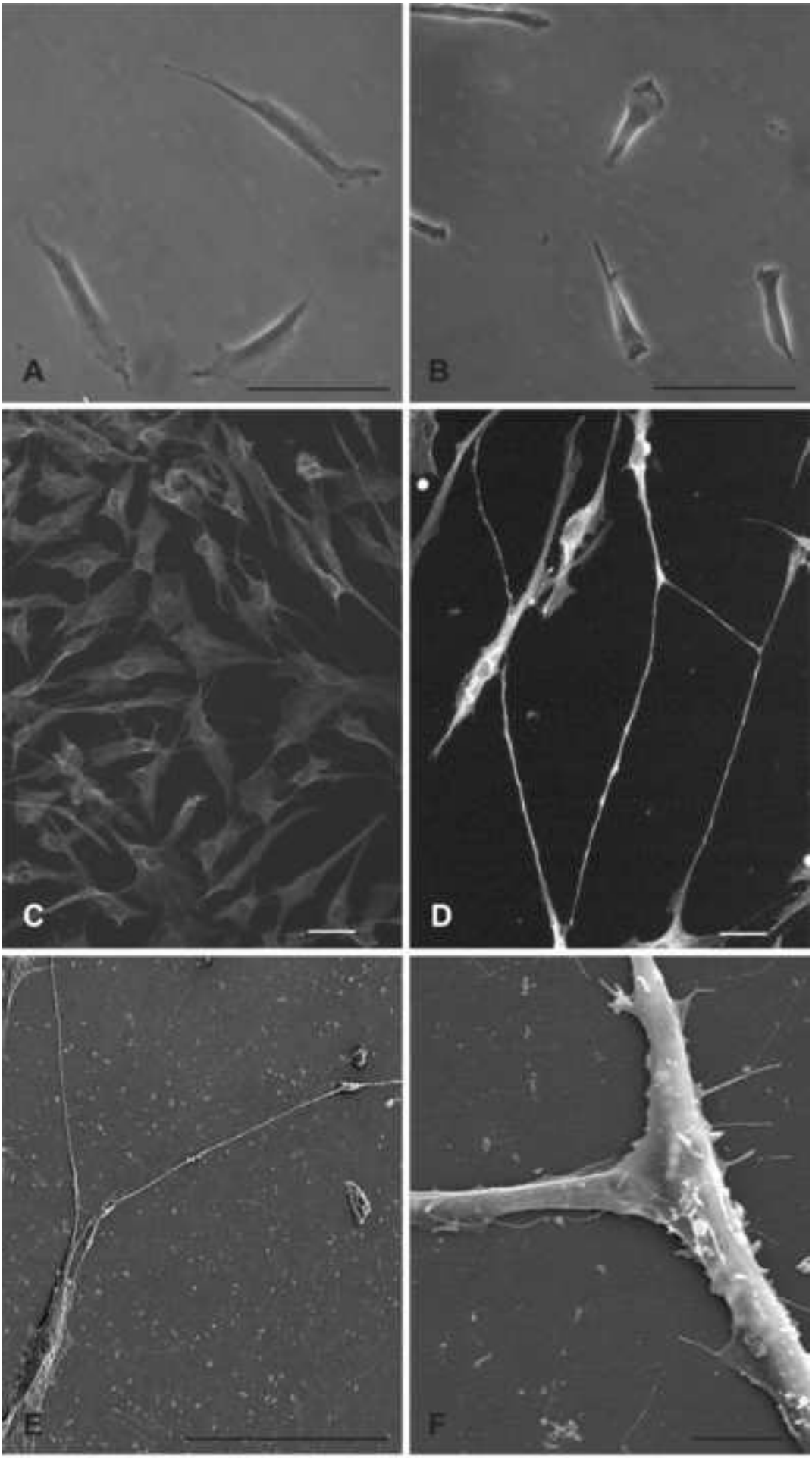

Figure 6

Click here to download high resolution image

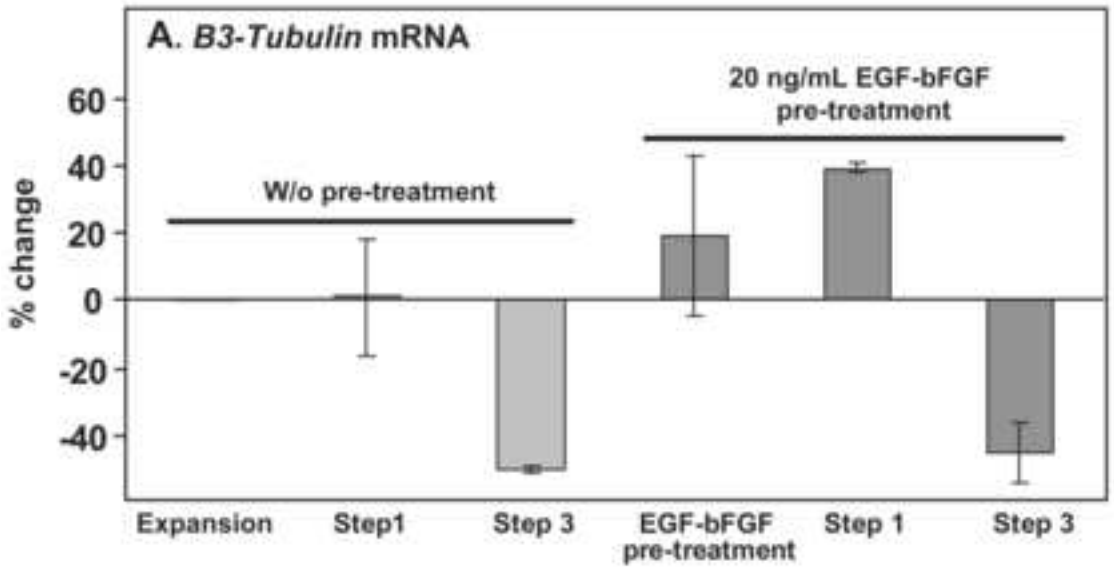

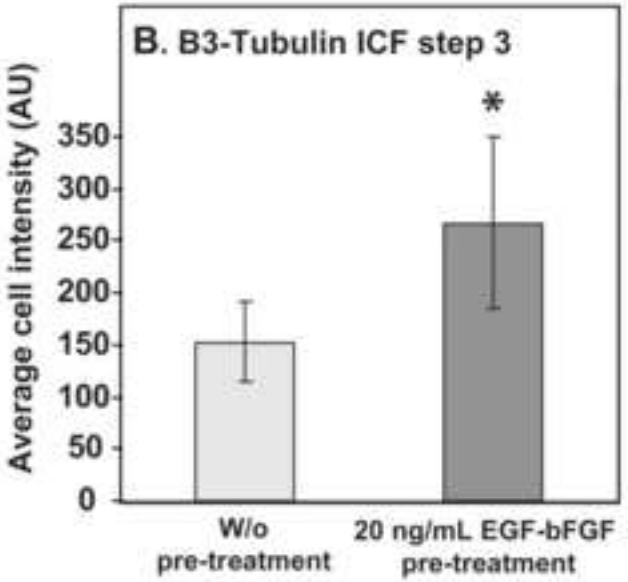

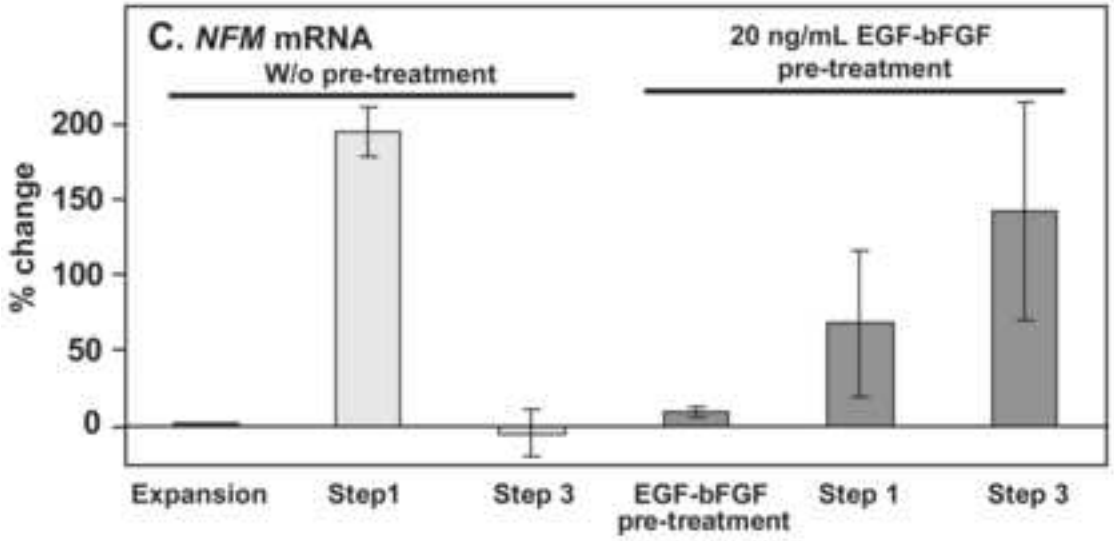

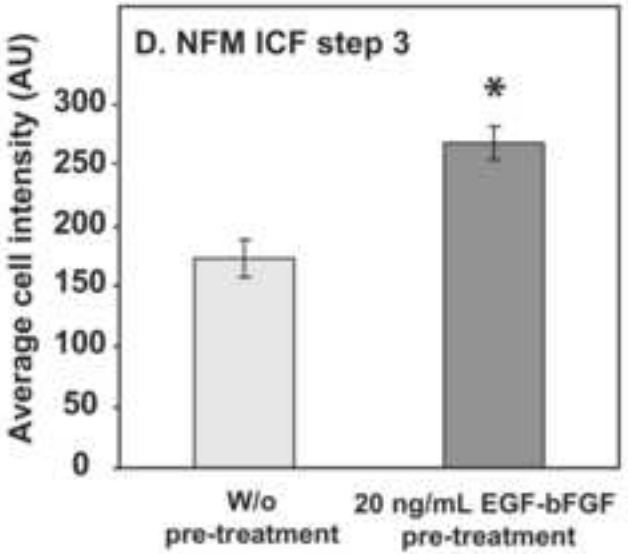

E. Increase in the percentage of positive cells with neuronal morphology at step 3 after EGF-bFGF pre-treatement

B3-Tubulin	120 %
NFM	250 %

Figure 7

Click here to download high resolution image